© Copyright 2008
Ting Li

The Extension of the Vitality Model and Its Application

Ting Li

A thesis
submitted in partial fulfillment of the
requirements for the degree of

Master of Science

University of Washington

2008

Program Authorized to Offer Degree:
Quantitative Ecology and Resource Management

University of Washington
Graduate School

This is to certify that I have examined this copy of a master's thesis by

Ting Li

and have found that it is complete and satisfactory in all respects,
and that any and all revisions required by the final
examining committee have been made.

Committee Members:

_____

James J. Anderson

_____

Vincent F. Gallucci

Date:_____

In presenting this thesis in partial fulfillment of the requirements for a master's degree at the University of Washington, I agree that the Library shall make its copies freely available for inspection. I further agree that extensive copying of this thesis is allowable only for scholarly purposes, consistent with "fair use" as prescribed in the U.S. Copyright Law. Any other reproduction for any purposes or by any means shall not be allowed without my written permission.

Signature _____

Date _____

University of Washington

Abstract

The Extension of the Vitality Model and Its Application

Ting Li
Chair of the Supervisory Committee:
Professor James J. Anderson
Quantitative Ecology and Resource Management

Anderson (2000, 2008) developed a model of vitality to characterize the properties of survival system. In this thesis, I extend to Anderson's vitality model by adding initial distribution to vitality, which makes the model more realistic. A Gaussian and gamma initial distribution are discussed here. A new algorithm for estimating parameters based on simulated annealing is presented, which allows us to explore the properties of population through their vitality parameters. Comparisons of the refined model and Anderson's model based both on simulation and real animal survival data leads to an issue of model selection. Finally, the model is applied to human survival data, leading to insights related to survival improvement and mortality plateau.

Table of Contents

List of Figures

Figure Number Page

List of Tables

Table Number Page

Introduction

Individuals even within a population are different at birth and differentiate further over time because of their unique experiences and innate capabilities. These differences are generically attributed to heterogeneity, which is an important factor in determining features of population survival. These include the time to starvation, response to stress, expected life span and mortality plateaus which is a widely observed tendency for mortality level off or even decline at old ages (Carey et.al 1992, Vaupel et.al 1994, 1998). In the biological context of survival analysis, one of the most important organizing principles is adaptive evolution by natural selection that rests on heterogeneity: genetic variation, differential survival or reproduction. Unlike evolutionary theories of demography, the lifelong heterogeneity theories related to mortality do not rest upon such well-established principles of biology. For a long time, survival models lacked a mechanistic basis for incorporating heterogeneity. The classical population-level models, which are usually described by differential equations, express mortality in terms of rates acting on homogeneous among a category. Thus, it makes this kind of models incapable of capturing the large variations between individuals. An alternative method is to use an Individual Based Model (IBM) tracking population traits at individual level. However, IBMs also lack a standard way to represent the variation and are often difficult to calibrate with the limited data available on population dynamics.

Recently, many new survival models have been developed to describe a demographic stochasticity in which variability in survival and reproduction rates are expressed as random events within population age classes (e.g., May 1973; Fox and Kendall 2002; Engen et al.2003; Boyce et al. 2006; Lande et al. 2006). They all somehow discuss the need to consider heterogeneity explicitly. In their opinion, mortality plateau is the result of statistical variation among a population in which weak individuals die at early ages while strong ones survive longer, finally leading to a decline of mortality rate at old ages. Heterogeneity may be expressed in the mortality rate of a Gompertz model by identifying individual rate coefficients of subpopulations (Yashin 2001, Service 2000). They did realize the importance of heterogeneity, however, their approaches are problematic because, once deaths occur, the hazard composition of a heterogeneous sample changes (Zens and Peart 2003). The issue is not trivial. The level of biases in interpreting models and data depend on how heterogeneity is formulated. Also, they classify heterogeneity in a way of genetic variation and environmental variation (Service 2000). Those definitions make it very hard to separate one kind of variation from the other especially when both are evolving with time. Last but not least, those models do not explicitly considers the processes that produce heterogeneity, and how the population structure changes as the individuals grow and die. Therefore, they cannot well explain the hidden mechanism with which we are mainly concerned.

Generally speaking, what we are concerned with is how to properly embed

heterogeneity into a survival model, so that it can help to clarify the internal mechanisms that lead to death. In our research context, heterogeneity among population is represented in one of two ways. The *existing variation* is the variation that is observed at a given time and is due to genetic heterogeneity and differences in life experience before the observation. The other is *evolving variation* which is developed as the individuals grow old and are exposed to variable environments after the observation. If the observation time is made at birth day, existing variation is due only to intrinsic or genetic differences, while evolving variation reflects subsequent differentiation. Existing variation describes a kind of static heterogeneity, while evolving variation reflects how a population becomes more heterogeneous with time due to variable experiences. It is believed that both of these are very important in mortality modeling, especially when the goal is not only to fit data, but to explore the real process of heterogeneity evolving with time. An idea survival model should be able to capture both heterogeneities.

For representing the latter variation, a totally new vitality model of fitting survival curves was initially published in a paper by Anderson in 1992 and further expanded in 2000 (See model detail in Appendix A: Background on Vitality Model). The vitality model for survival is a method that characterizes the complex interactions between external and internal processes by a quantity called “vitality” which denotes the remaining survival capacity of an organism. Each individual begins with an initial vitality, v_0, and dies when its vitality reaches zero (fig. 1). The random trajectory of

vitality, v, between v_0 and 0 is described by the Wiener process:

$$dv/dt = -\rho + \sigma\varepsilon_t \quad (1)$$

where ρ is the mean value of the rate of vitality loss, σ is the magnitude of the stochastic component.

The two parameters ρ and σ are set to be constant within a population level. Then an analytical solution is obtainable if at t=0 the population distribution is homogeneous, i.e. with all the individuals having the same initial vitality v_0. Thus, a survival model is expressed (Anderson 2000):

$$l(t) = l_v(t)l_a(t) = \left(\Phi\left(\frac{1}{s\sqrt{t}}(1-rt) \right) - \exp\left(\frac{2r}{s^2} \right) \Phi\left(-\frac{1}{s\sqrt{t}}(1+rt) \right) \right) \exp(-kt) \quad (2)$$

Where $l(t)$ is the survival rate and $r = \rho/v_0$, $s = \sigma/v_0$ are normalized drift and variation parameters respectively. $\Phi(g)$ is the cumulative distribution function of normal distribution. Then

$$l_v(t) = \left(\Phi\left(\frac{1}{s\sqrt{t}}(1-rt) \right) - \exp\left(\frac{2r}{s^2} \right) \Phi\left(-\frac{1}{s\sqrt{t}}(1+rt) \right) \right) \quad (3)$$

gives the vitality-based survival and

$$l_a(t) = \exp(-kt) \quad (4)$$

is the accidental mortality related survival described by a Poisson process where *k* is the accidental mortality rate. Model described by eq. (2) is called a Dirac delta model since the initial distribution starts as Dirac delta function with point source or a 3-parameter model determined by *r*, *s* and *k*.

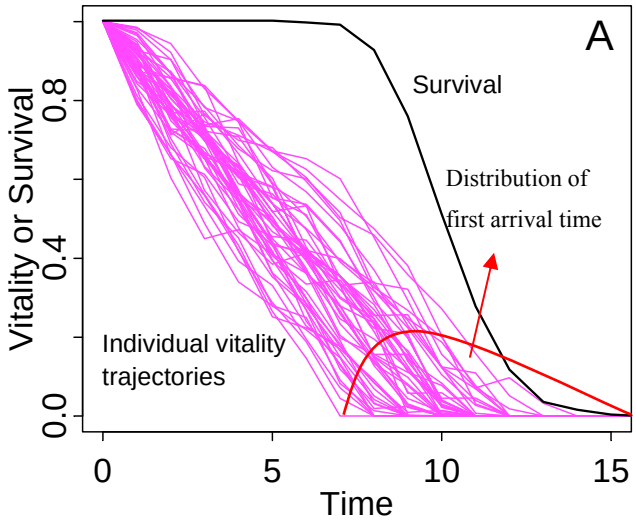

Figure 1: Depicts individual vitality trajectories (eq. (1)) and survival (eq. (3)).

The heterogeneity is described as the variation of vitality evolving with time. As stated above, there are two basic assumptions for this model, the constant vitality parameters r and s, and identical starting point for initial vitality within a population. This model provides a reasonable characterization of heterogeneity in survival. But because of the assumption of identical initial condition, the existing variance mentioned above is not accounted for in this model.

The limitations of Anderson's model

Early as 2004, Steinsaltz and Evans (2004) pointed out the limitations of Anderson's

model with a statement that convergence and other properties of models that relied on Weiner processes may depend on initial distributions. The hazard rate in this mortality process is shaped by the initial distribution and the way it slowly fades away. More importantly, they concluded that the fundamental question in biodemograhy, the mortality plateau, has something to do with the quasistationary distribution whose shape is determined by the initial distribution. Quasistationay distribution is the limiting distribution that the process will gradually approach and is a generic feature of Markov model (Aalen and Gjessing 2001, Steinsaltz and Evans 2007). When a process reaches its quasistationay distribution, it will have a constant hazard rate of transition. This means that although the probability mass is continuously being drained from the transient space, nevertheless the remaining probability distribution on this space converges to a limiting distribution (Aalen and Gjessing 2001). That stage of constant hazard corresponds to the mortality plateau. Steinsaltz and Evans (2004) showed that, given enough time, and under certain conditions, the transient state will converge to the quasistationary distribution regardless of the initial distribution. And the initial distribution will determine the shape of the limiting distribution. Thus, the assumption of identical initial distribution may not only violate the reality of a natural population but also fail to reveal some important properties that particularly help to understand how the heterogeneity evolves as well as the fundamental question pertaining to mortality plateau.

Anderson's model has been applied to many survival data of different animal species.

Although the model fits most of data well, it has difficulties capturing the early life curvature for some species. Fig. 2 gives an example of the model fitted to fruit fly survival data from Carey's study of *Ceratitis capitata* (1998). We fell that it fit poorly in the early life stages because it does not account for initial variation. Anderson et al. (2008) also applied this model to a study of starvation time of yellow perch (Letcher et al. 1996). Different treatments (starvation) were used to predict survival through vitality parameters. Fish are divided into three groups by size. For the first two groups with smaller size, prediction equations developed from Anderson's model seem to fit data well, but they fail for the fish group of large size. One possible explanation of this undesirable performance is the neglect of initial variation existing at the beginning of treatment stage. We believe that large size group fish are more heterogeneous than the other two groups initially, thus the 3-parameter model is not able to capture the big initial heterogeneity. To solve this problem, it is necessary to consider extensions of this basic vitality model by weakening the assumptions and integrating initial variation into it.

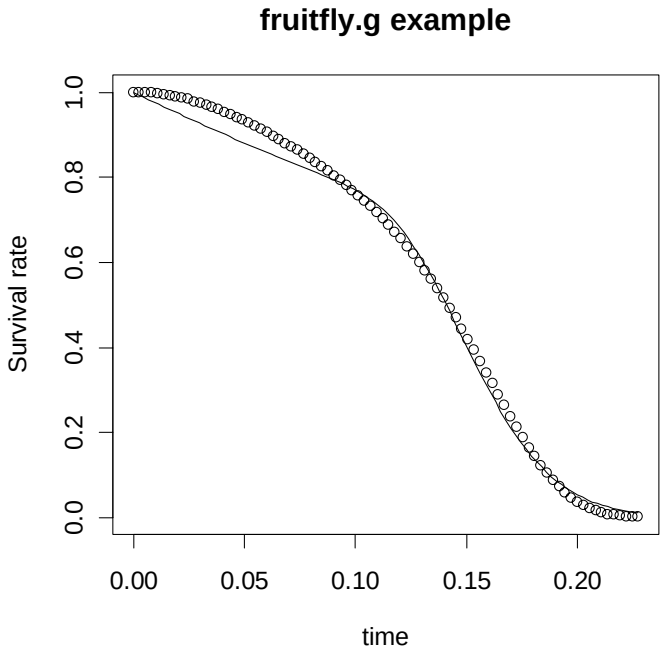

Figure 2: Anderson's model fits to a fruitfly survival data from Carey's study of Ceratitis capitata (1998)

It is the goal of my work to present several extensions of Anderson's vitality model that account for further heterogeneity and to develop routines that are able to estimate parameters for quantifying the roles of heterogeneity and intrinsic change in determining vitality distribution and, consequently, the final survival rate.

Chapter I: Introducing Initial Vitality Distribution

Vitality distribution

Since heterogeneity is represented through vitality, I begin by discussing the vitality distribution. At a given time t, the probability of a vitality v given the initial vitality v_0 is defined by equation (3) as derived from the Wiener Process, equation (1), (Chhikara and Folks 1989). Death is represented by an absorbing boundary at $v = 0$, which represents the removal of individuals from the cohort at the zero boundary.

$$p_v(v,t \mid v_0,0) = \frac{1}{\sigma\sqrt{2\pi t}}\left[\exp\left(-\frac{(v-v_0+\rho t)^2}{2t\sigma^2}\right)-\exp\left(\frac{2\rho v_0}{\sigma^2}-\frac{(v+v_0+\rho t)^2}{2t\sigma^2}\right)\right] \quad (5)$$

Previously (Anderson 2000, 2008), a Dirac delta function was assigned to initial vitality v_0 which guaranteed all individuals in the cohort get the same initial vitality. This is not realistic, since a combination of genetic variation and variable prenatal conditions cause organisms to be intrinsically different even at birth. Therefore, we introduce an initial distribution for vitality.

In order to import reasonable and meaningful initial distribution, one must first understand which distributions are likely. Since the vitality density (3) evolves from a Dirac delta function spike, first spreads into a Gaussian-like shape, and then into a quasi-stable gamma-like distribution that is finally absorbed into the zero-vitality boundary (Aalen and Gjessing 2001) (fig.3), the Gaussian and gamma distribution are good choices for the initial distribution v_0 that complements the natural evolution of

vitality. If the beginning time of observation is picked up as an early time of a cohort, the initial vitality tends to be normal like. The gamma distribution implies more asymmetry among a population: with death occurring, most individuals have low vitality while a few have high vitality. This usually occurs at a later time, when death has "filtered" a population. Below, we'll focus on those two kinds of initial vitality distributions and understand how they affect the resulting survival curve.

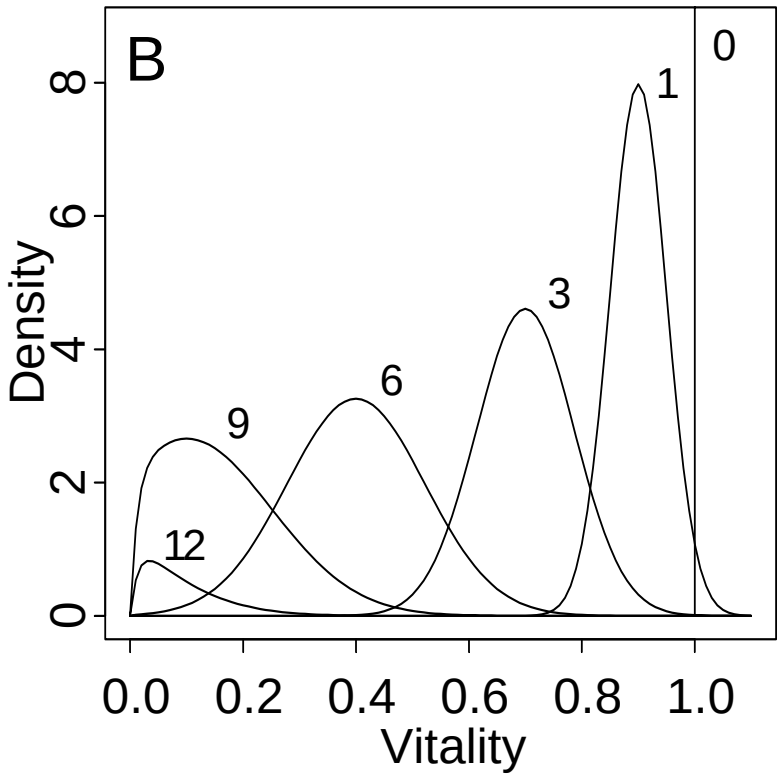

Figure 3: vitality distribution evolving with time. In eq. (5) vitality density evolves from a Dirac distribution at day 0 into a Gaussian distribution over days 2 through 6 and into a gamma-like distribution by day 9. With time, the area under the curve diminishes by loss of vitality into the zero-boundary

General framework for including an initial distribution

Basically, there are two approaches that could be used to derive the vitality based

survival function from the Wiener process. One is based on the first arrival time, while the other one is directly derived from the vitality distribution.

An important result known about the Wiener process is the distribution of times when the process first hits zero. This is referred to as the first arrival time distribution (fig.1). According to our definitions, survival rate at time t is just the survival fraction of total population at time t, and is equivalent to the probability that the individual vitality does not hit zero by time t. Since the cumulative density function of first arrival time $F(t)$ gives the probability that individual vitality hits zero by time t, the vitality based survival rate $l_v(t)$ is expressed as:

$$\begin{aligned} l_v(t) &= 1 - F(t) \\ &= 1 - \int f(t)dt \\ &= 1 - \int f(t \mid v_0)\, p(v_0) dv_0 \end{aligned} \tag{6}$$

Here $f(t)$ is the marginal distribution of first arrival time while $f(t \mid v_0)$ is the conditional distribution, and $p(v_0)$ is the initial distribution of v_0.

The conditional distribution of first arrival time:

$$f(t \mid v_0) = \frac{v_0}{\sigma\sqrt{2\pi}} t^{-2/3} \exp\left(-\frac{(v_0 - \rho t)^2}{2\sigma^2 t} \right) \tag{7}$$

is an inverse Gaussian distribution derived directly from Wiener Process eq.(1) . (Aalen and Gjessing 2001)

The other method directly from the vitality distribution is relatively simple and easily to be understood. $l_v(t \mid v_0)$ is actually the conditional distribution by introducing initial vitality to non-normalized version of eq. (3). Then the marginal probability is given by integrating v_0 from 0 to infinity,

$$l_v(t) = \int l_v(t \mid v_0)\, p(v_0) dv_0 \tag{8}$$

Initial Gaussian distribution

We consider introducing a Gaussian initial distribution for vitality in this section that assumes: $v_0 :\ N(\mu, \tau^2)$. Here we adopt the first method using first arrival time, because we are able to get an analytical solution from this method.

$p(v_0) = \frac{1}{\sqrt{2\pi}\tau} e^{-\frac{(v_0-\mu)^2}{2\tau^2}}$, which is normally distributed here. Then following eq. (6) and (7),

$$\begin{aligned} f(t) &= \int f(t \mid v_0)\, p(v_0) dv_0 \\ &= \int \frac{v_0}{2\pi\sigma\tau} t^{-3/2} \exp\left(-\frac{(v_0 - \rho t)^2}{2\sigma^2 t} - \frac{(v_0-\mu)^2}{2\tau^2} \right) dv_0 \\ &= \frac{\tau^2\rho + \sigma^2\mu}{\sqrt{2\pi}} (\tau^2 + \sigma^2 t)^{-3/2} \exp\left(-\frac{(\mu - \rho t)^2}{2(\tau^2 + \sigma^2 t)} \right) \end{aligned} \tag{9}$$

Together with eq. (6) and (9):

$$l_v(t) = 1 - F(t)$$

$$= \Phi\left(\frac{\mu - \rho t}{\sqrt{\tau^2 + \sigma^2 t}}\right) - \exp\left(\frac{2\tau^2\rho^2}{\sigma^4} + \frac{2\mu\rho}{\sigma^2}\right)\Phi\left(\frac{-\frac{2\tau^2\rho}{\sigma^2} - \mu - \rho t}{\sqrt{\tau^2 + \sigma^2 t}}\right) \quad (10)$$

Let $r = \frac{\rho}{\mu}$, $s = \frac{\sigma}{\mu}$ and $u = \frac{\tau}{\mu}$ (11)

$$l_v(t) = \Phi\left(\frac{1 - rt}{\sqrt{u^2 + s^2 t}}\right) - \exp\left(\frac{2u^2 r^2}{s^4} + \frac{2r}{s^2}\right)\Phi\left(\frac{-\frac{2u^2 r}{s^2} - 1 - rt}{\sqrt{u^2 + s^2 t}}\right) \quad (12)$$

is the vitality based survival rate with normalized parameters where r, s and u are normalized parameters and u represents the standard deviation of the initial distribution of vitality which is a totally new parameter.

It should be noted that when we calculate the marginal distribution of $f(t)$, v_0 is integrated over the whole real space from minus infinity to plus infinity instead of just positive line, which violates the biologically meaningful assumption that vitality should be positive. Thus, the estimates of parameters might be biased when the initial standard deviation of v_0 gets big. For small u, eg. (0, 0.35), most (over 95%) individuals drawn from distribution $v_0 : N(1, u^2)$ have positive initial vitality v_0, indicating that we generally do not need to be worried about bias in this situation. Figure 4 below shows clearly that skewness happens when u is bigger than 0.35. Moreover, when the standard deviation is beyond 0.35, we tend to believe a gamma initial distribution would be more proper here. This observation, however, also

suggests that the initial Gaussian distribution is transitioning to gamma naturally and it is necessary to consider both distributions. We will further discuss the connection between those distributions and their effect on the survival curve. Also, this bias caused by inappropriate integrating range is discussed in the section of simulation.

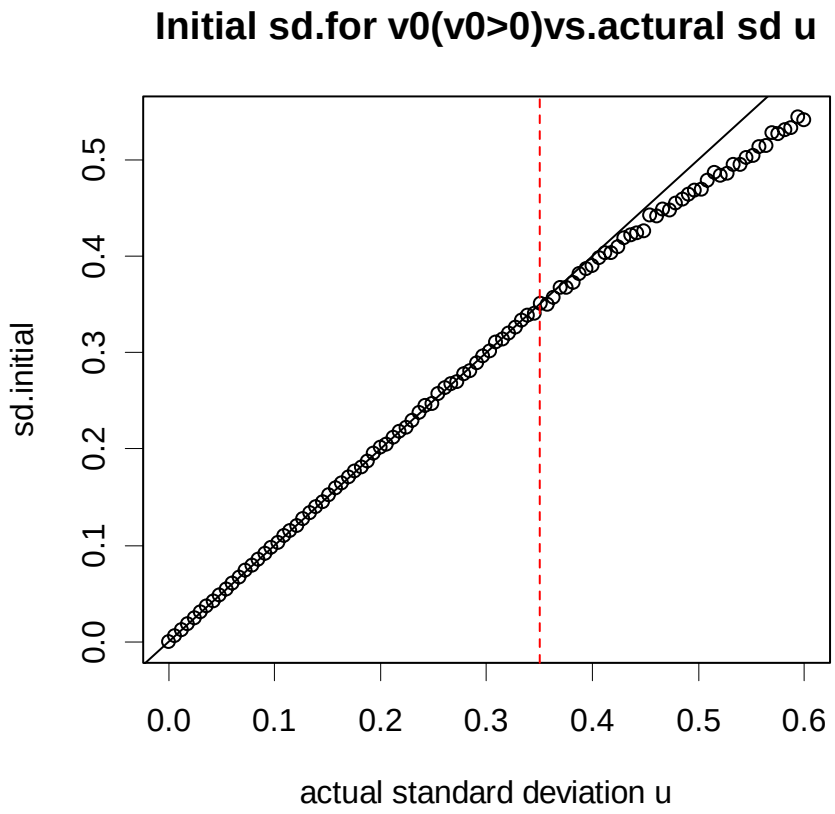

Figure 4: initial standard deviation for v_0 (truncating at v_0>0) vs. actual standard deviation u from initial Gaussian distribution

Initial gamma Distribution

A gamma distribution for v_0 is considered in this section. Unlike the initial Gaussian distribution, there is no explicit form for the marginal distribution of first arrival time and vitality density. Therefore we need to use different methods. We use the second

approach mentioned before that derives the equation directly.

In a non-normalized version of equation 3), vitality-related survival rate is expressed as:

$$l_v(t) = \left(\Phi\left(\frac{1}{\sigma\sqrt{t}}(v_0^* - \rho t) \right) - \exp\left(\frac{2\rho v_0^*}{\sigma^2} \right) \Phi\left(-\frac{1}{\sigma\sqrt{t}}(v_0^* + \rho t) \right) \right) \quad (13)$$

here v_0^* denotes the initial vitality.

The parameters are normalized by dividing the mean of initial vitality v_0^*. That is,

$r = \rho / \overline{v}_0^*, s = \sigma / \overline{v}_0^*$ and $v_0 = v_0^* / \overline{v}_0^*$:

$$l_v(t \mid v_0) = \left(\Phi\left(\frac{1}{s\sqrt{t}}(v_0 - rt) \right) - \exp\left(\frac{2rv_0}{s^2} \right) \Phi\left(-\frac{1}{s\sqrt{t}}(v_0 + rt) \right) \right) \quad (14)$$

In this scenario, $v_0 = v_0^* / \overline{v}_0^*$ is assumed to have a gamma distribution with mean equal 1: $v_0 \sim gamma(shape = w, scale = u^2)$. To have the restriction of mean, $u^2 \times w = 1$. Thus, w is set to be $1/u^2$. It is noticed that by definition, the normalized standard deviation of initial vitality for gamma model is $\left[\left(1/u^2 \right) \times u^4 \right]^{1/2} = u$, and the non-scaled standard deviation of initial vitality τ equals $u \times \overline{v}_0^*$, which is consistent with Gaussian model.

$$
\begin{aligned}
l_v(t) &= \int l_v(t \mid v_0)\, f(v_0) dv_0 \\
&= \int \left(\Phi\left(\frac{1}{s\sqrt{t}}(v_0 - rt) \right) - \exp\left(\frac{2rv_0}{s^2} \right) \Phi\left(-\frac{1}{s\sqrt{t}}(v_0 + rt) \right) \right) gamma(v_0, 1/u^2, u^2) dv_0 \qquad (15) \\
&= \int \left(\Phi\left(\frac{1}{s\sqrt{t}}(v_0 - rt) \right) - \exp\left(\frac{2rv_0}{s^2} \right) \Phi\left(-\frac{1}{s\sqrt{t}}(v_0 + rt) \right) \right) v_0^{1/u^2 - 1} \frac{(1/u^2)^{1/u^2} e^{-v_0/u^2}}{\Gamma(1/u^2)} dv_0
\end{aligned}
$$

Unfortunately, there is no explicit form for the integral; however, we can estimate the parameters numerically.

Still, I need to point out the restriction I put on the initial gamma distribution of v_0 would not lose any generality. We assume the normalized initial vitality $v_0 \sim gamma(shape = 1/u^2, scale = u^2)$ with mean equaling 1 and standard error equaling u. Then, the original $v_0^* = \overline{v}_0^* \times v_0$ implies $v_0^* \sim gamma(shape = 1/u^2, scale = \overline{v}_0^* \times u^2)$ with mean equaling $\overline{v}_0^*$ and standard error equaling $\overline{v}_0^* \times u = \tau$. Actually, $\overline{v}_0^*$ and τ could be any reasonable values. (see Appendix B).

Together with accidental survival part, total survival function equals $l(t) = l_v(t) l_a(t)$ (16) for both Gaussian and gamma initial distribution and $l_a(t) = e^{-kt}$ is the same as that in Anderson's 3-parameter model.

This new survival function incorporating initial vitality distribution has four parameters including *r, s, k* and *u*. So it is called 4-parameter model distinct from the original 3-parameter model. Or we can call them Gaussian model and gamma model

separately comparing to the name of Dirac delta model.

Effects of different initial vitality distribution on survival curve

Now, we have two models, an initial Gaussian distribution model and an initial gamma distribution model. (The original 3-parameter model is a special case of initial Gaussian model setting $u = 0$.) Fig. 4 below could well explain their different effects to shape a survival curve. r, s and k are set to be the same for the two models, u is within a range of 0 to 0.35 for Gaussian model and a range of 0.35 to 0.7 for gamma model.

As the model changes from a Gaussian initial to a gamma initial, the survival curve becomes steeper in the beginning and flatter in the end, and different curves crossed each other around the 35% mortality time. Fig.5 shows that a population with large initial variance will be frailer at early times, but have higher survival at older ages as comparing to a small initial variance population. Also notice that the curve from Gaussian model with $u = 0.35$ is very close to the gamma model with $u = 0.35$ which makes much sense, since a gamma model with small u tends to have a normal-like shape similar to that of Gaussian model at $u = 0.35$. This result supports the former hypothesis.

Fig. 6 gives another way to look at the relationship between the initial variation and the survival rate by fixing the time. That is each line in fig. 6 represents the change of survival rate at a given time as a function of u, the standard deviation of initial

distribution. In order to compare the behavior, lines are drawn from both Gaussian initial and gamma initial model with u ranging from 0 to 0.7. Clearly, for earlier age (t=10), survival rate from both models declines with increasing u, while for later age (t=40), the trend reverses. And at middle age (around time 22), the lines are relatively flat, indicating the contribution of different initial variation to middle age survival is difficult to differentiate. All of the information reported above is essentially the same as fig. 5 that small initial variation favors early age population but becomes less beneficial for old age population. What're new in fig. 6 are the differences between the lines from Gaussian model and those from gamma model, especially when u is large. It appears that the line from Gaussian is below gamma line at early age, but turns to be above gamma line at middle age, although there is no big difference at old age. As it has been discussed before, bias affects the Gaussian model at large values of u. This again underlines the preferability of using gamma initial distribution. We still prefer to use Gaussian model for small u is because it is much easier to calculate Gaussian model than gamma model. This will be further discussed in the next chapter.

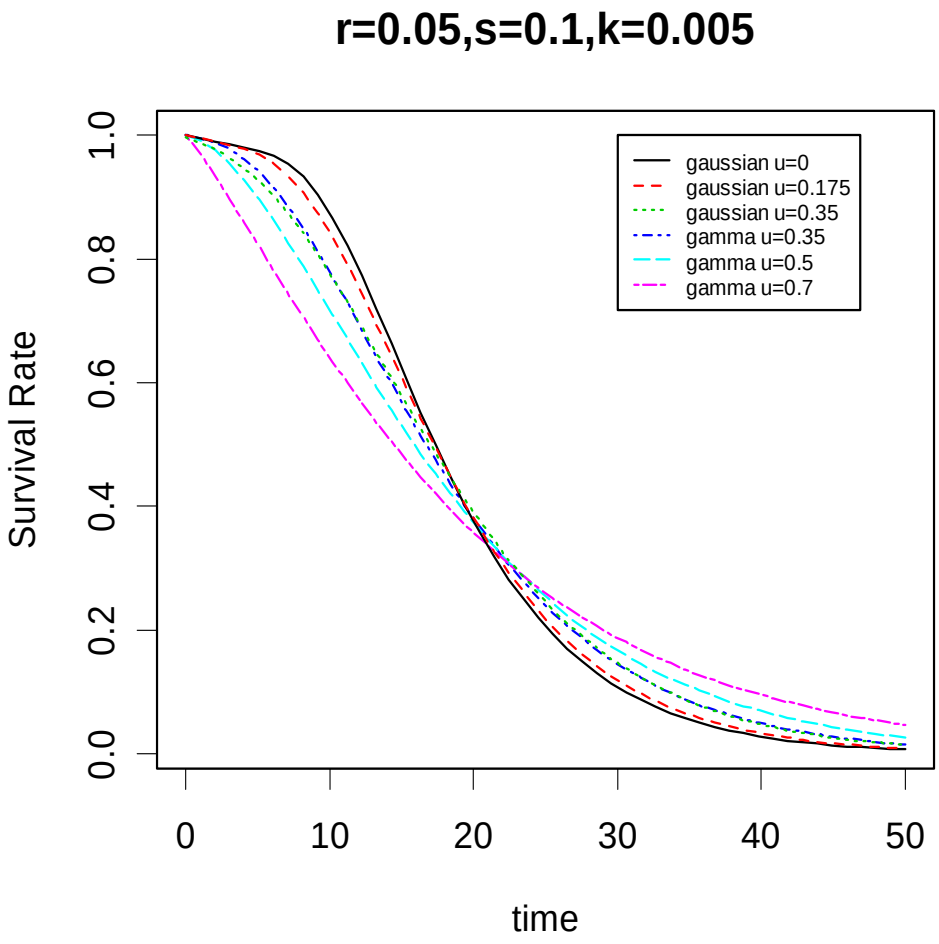

Figure 5: Survival curves from Gaussian and gamma model with different initial stand deviation parameters.

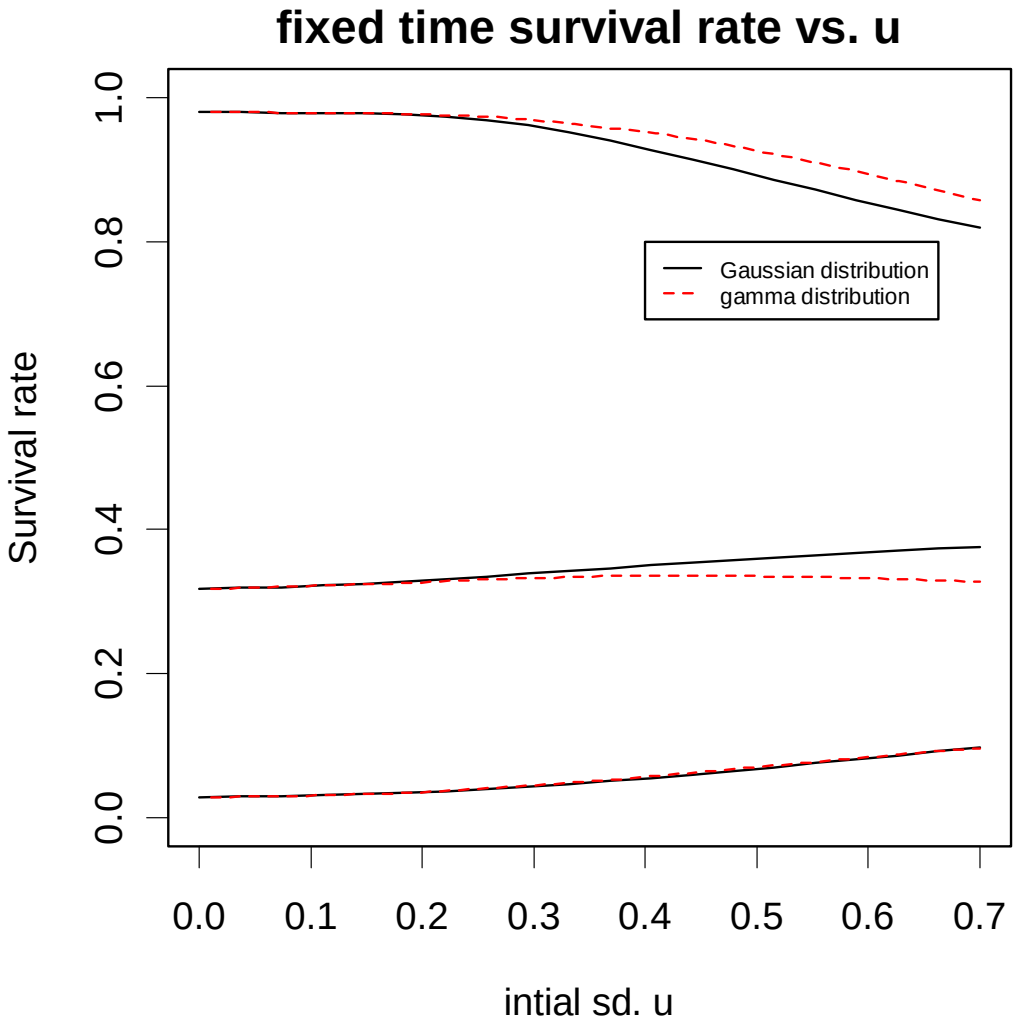

Figure 6: Fix time survival rate. Survival rate changes with initial standard deviation at fixed time point for initial Gaussian and gamma distribution separately. The upper lines are at time 10, the middle ones are at time 22 and the bottom ones are at time 40. Solid line: Gaussian initial distribution, dash line: gamma initial distribution. This curve can not be generated entirely from fig. 5.

Chapter II: Parameter Estimation and Model Selection

In this chapter, we develop a routine to estimate the four parameters of model (eq. (16)). For a given survival curve, the goal is to derive the values of parameters that provides the best fit to the curve. If the survival rate is changed into a likelihood function, the problem becomes an MLE optimization. For the former 3-parameter model (eq. (2)), Salinger et al. (2003) developed a routine based on Newton-Ralphson method. However, this method is highly dependent on the choice of initial parameter values since it is easy to fall into a local minimum instead of a global optimal solution. Salinger et al. successfully established a constraint equation for the initial values using the time to 50% mortality. However, this approach fails when it is applied to the new model, and an alternative optimization method is required. Currently, one of the popular well-developed approaches that could be used for searching global optimization is simulated annealing (Kirkpatrick et al., 1983). I choose to use it and it does produce good estimates for the 4-parameter models.

Another issue with much survival data is that it is interval-censored; that is the mortalities are counted at the end of each time period rather than continuously. Salinger et al (2003) dealt with this issue by considering the incremental mortality probability as the likelihood function. We choose to retain their approach. Salinger et al (2003) estimated standard errors by examining the estimated variance matrix. Specifically, standard errors are obtained by taking the square root of the diagonal elements in the inverse of the Hessian of the negative log-likelihood, evaluated at the

parameter estimates (cf. Kendall and Stuart, 1997, Section 18.26).

Simulated Annealing

Simulated annealing was developed by Kirkpatrick et al. (1983). It is a Monte Carlo method introduced by Metropolis et al. (1953) based on the theory of statistical mechanics. The idea comes from a process of condensed matter physics in which a solid material in melded to a liquid phase and then slowly cooled. The heating arranges the molecules randomly and the cooling rearranges them into a perfect crystal. Application of simulated annealing to optimization problems is based on the analogy between the state of each molecule and the state of each parameter that affects the energy function (analogous to the cost function in the optimization problem) to be minimized. The parameter values are randomly perturbed, and the probability of accepting the perturbed cost function is determined by the Metropolis criterion,

$$P(\Delta\Phi) = \begin{cases} 1 & ,if\ \Delta\Phi \le 0 \\ e^{-\frac{\Delta\Phi}{T}} & ,otherwise \end{cases} \qquad (17)$$

where $\Delta\Phi$ is the change in the cost function due to the perturbation, and T is the current system temperature, which is a control parameter. To be specific, $\Delta\Phi = f(new\ \ parameters) - f(old\ \ parameters)$, where f is the cost function to be minimized. As the search iterations progress, the temperature parameter T is reduced according to what is known as the "temperature schedule". Providing that the starting

maximum temperature is sufficiently high and the temperature T is lowered slowly, the algorithm is guaranteed to reach the global minimum or a point close to the global minimum of the cost function. However, the choice of temperature schedule including the star temperature and the way to lower it down is somewhat arbitrary and depends on the specific cost function. Find the most efficient schedule requires some experimentation.

Implementation of the simulated annealing algorithm is relatively straightforward. I follow the implementation described by Corana et al. (1987) and define constraints to insure that the parameters locate in their allowable range, like positive real line.

Fig. 7 shows a simplified flow chart of the modified simulated annealing algorithm. Starting with a given set of initial parameters and a high initial temperature T ($=10^3$), the cost function is then calculated and recorded. The current parameters are then randomly perturbed within the boundary, like choosing a random variable from uniform (0, 1) and then moving a step proportion to that variable. The cost function is computed, and the probability of accepting the new parameters is determined by eq.(17). After N_T ($10\times$ number of parameters) step adjustments, the temperature T is then reduced by a constant factor r_T (=0.85). The loop terminates when the differences between the recent N_ε (=4) values of minima are less than a tolerance $\varepsilon(=10^5)$ and the parameter changes are less than 0.1%. These criteria help guarantee that the global minimum is reached.

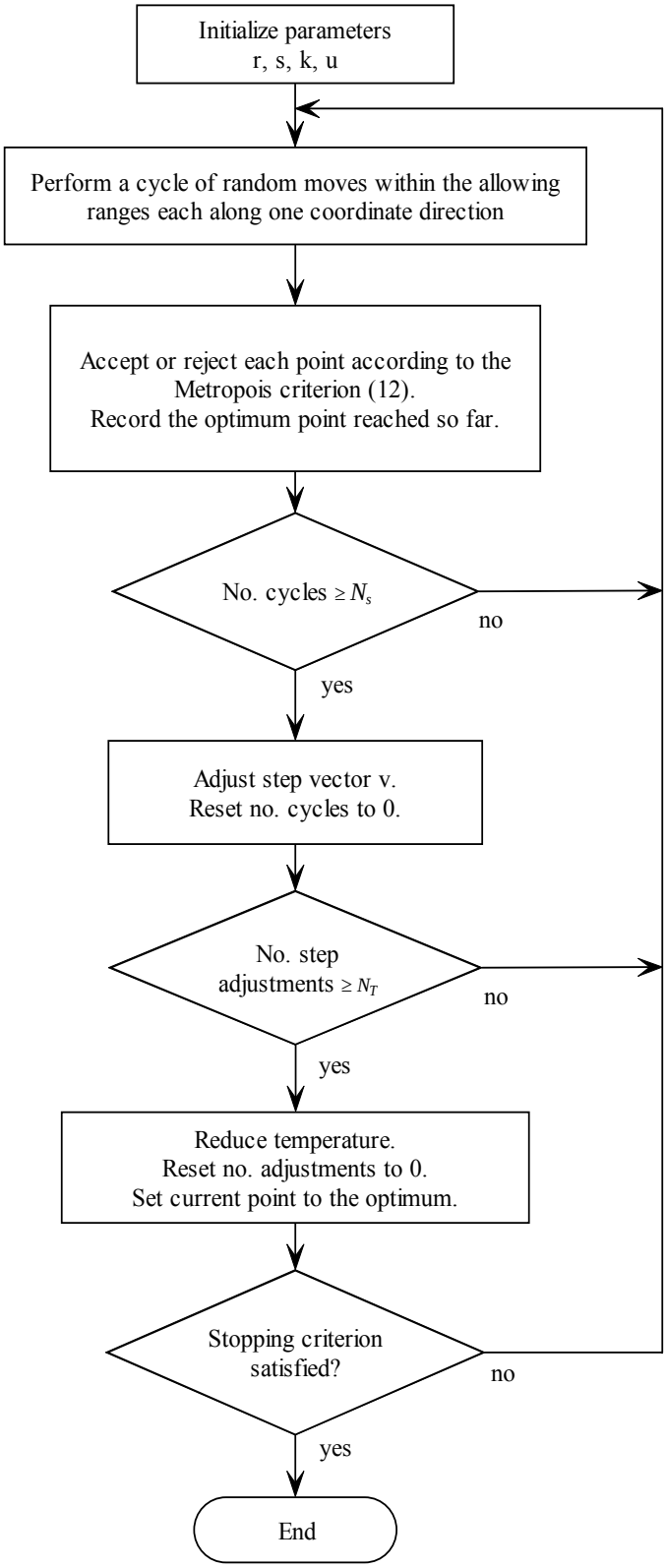

Figure 7: flow chart of simulated annealing.

Simulation and Model Comparison

To understand the fourth parameter u and evaluate the performance of the new 4-parameter models with initial Gaussian and gamma vitality distributions separately, I conducted simulations and compared results with the 3-parameter model based on AIC.

Each distribution is created using a vitality process. Each individual in a population was assumed to have a vitality v_0 at time 0, where v_0 is drawn from $N(1,u^2)$ and gamma (shape=$1/u^2$, scale=u^2) distribution for the Gaussian and gamma case respectively. The vitality for each individual was calculated for a single time step by the following equation.

$$v_t = v_{t-1} - r_a + s_a \times W \qquad \text{t=1,2,3....} \qquad 15)$$

where *W* is the white noise calculated by selecting a random number from a normal distribution. Death time t^* is recorded for each individual when v_t hits zero or an accidental mortality happens with a probability of 1-e^{-kt^*}. Thus, we have generated a survival curve for a population.

Each distribution represents a population with 10000 members. The r value used to generate the distributions is 0.05, and the s and k value are controlled as 0.1 and 0.005 separately. Finally, we allow u to range from 0.01 to 0.6 for Gaussian initial and from 0.4 to 0.7 for gamma initial distribution.

Simulation Results

Both table in Appendix C and fig. 8 below show the simulation results. The first 7 simulations are generated from Gaussian initial distribution with u from 0.05 to 0.5. It appears that the estimates of r and s are relatively similar to each other for 3- and 4-parameter models across all the 7 simulations. Among the range of u from 0.05 to 0.3, the parameters estimated by 4-parameter Gaussian model are close to the actual values, but bias becomes significant with the increase of u. As mentioned in the previous section, some bias is inevitable for Gaussian model due to the inappropriate range for the integration. Consistent with former discussion, parameter estimates from simulation behave relatively stable when u is less than 0.35, but bias dominates after then. Also, as the increase of initial variation, r decreases, but k is raised to compensate the bias from both r and u. At the same time, since the true initial distribution is Gaussian, although estimated r, s and k are close to the true values, the gamma model tends to overestimate u and performs not as good as the Gaussian model.

The last five simulations are from the gamma initial distribution with u equaling 0.4, 0.5, 0.577, 0.632 and 0.7 respectively. Apparently, in this situation, the gamma model fits data better than the other two models and parameters estimated from it are closer to the actual ones. Both 3-parameter and 4-parameter Gaussian models seem unable to capture the big initial variation, as values for r are decreased and values for k increased in order to obtain the fit.

I must point out the gamma model underestimates r and s across all values of *u*. The possible reason for this is that the numerical algorithm generating survival curves does not adequately represent the Brownian process. There is a slice different from the generating survival curve and the curve calculated from survival function directly. This discrepancy might be responsible for the underestimation.

Former work has shown that the vitality distribution evolving with time changes from a normal-like to a gamma-like distribution. It is indicated that the normal-like distribution corresponds to a spread term (standard deviation) ranging from 0 to 0.35 while a gamma-like distribution corresponds to a range of 0.35 to 0.7. Therefore, it is not surprising that the 4-parameter Gaussian model behaves better over a range of *u* from 0.05 to 0.3 under this explanation but loses to the gamma model when u is large. Introducing a gamma initial distribution for v_0 is one way to correct the bias as would be expected.

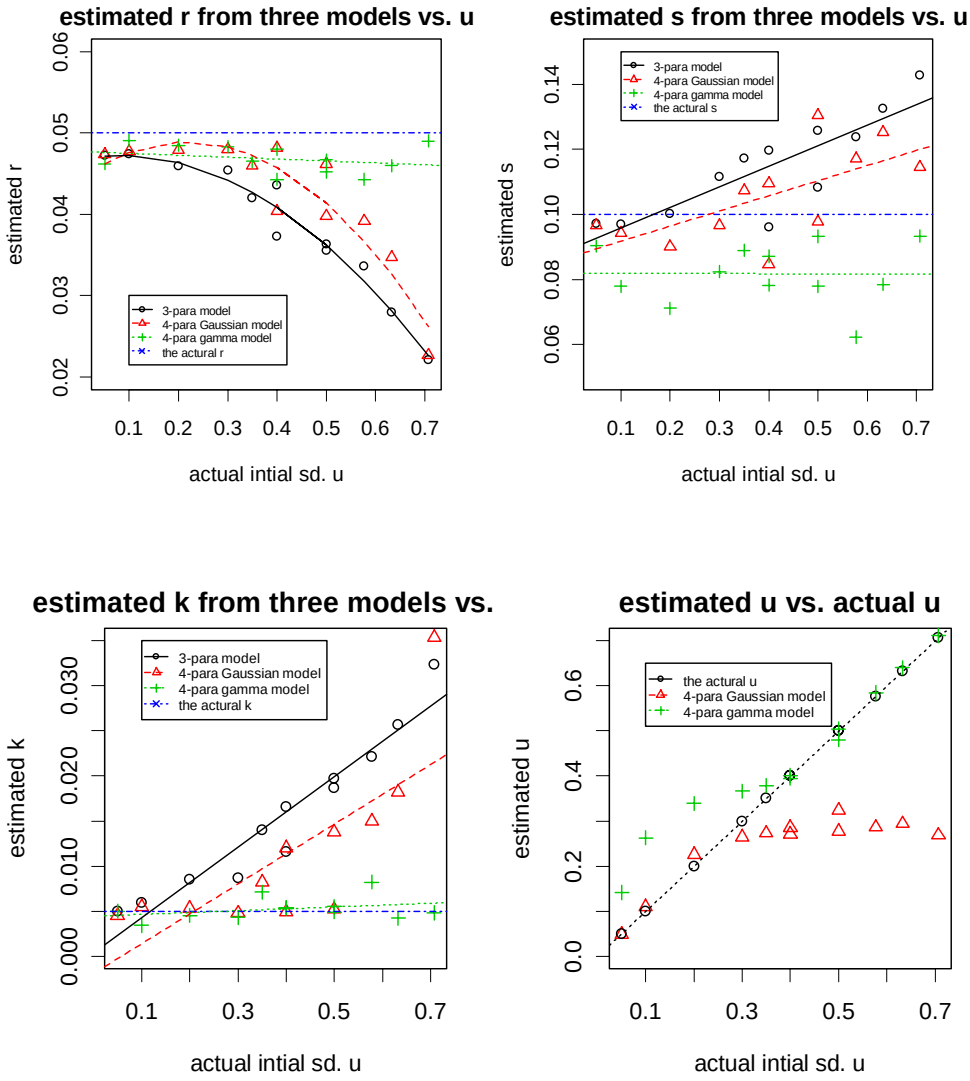

Figure 8: estimated parameters versus actual values of initial standard deviation u for 3-parameter model, 4-parameter Gaussian model and 4-parameter gamma model.

Model Comparison and Model Selection

From a purely mathematical view, AIC would be a good criterion to conduct model comparison and model selection. Based on AIC (Burnham and Anderson 2002) reported in Appendix C, among the range of small *u* (0-0.05), the 3-parameter model is good enough to capture the survival information, as indicated by the smaller AIC value compared to the 4-parameter models. But, as *u* increases, the 4-parameter

models outperform the 3-parameter model, as expected. Under the condition of true initial distribution of Gaussian, although bias turns out as the actual initial standard deviation *u* gets big, the Gaussian model still performs better than both 3-parameter model and gamma model. Furthermore, it appears that the bigger the *u* is, the better the Gaussian model performs over the 3-parameter model. When using gamma as the actual initial distribution of sampling, the gamma model unsurprisingly performs better than both the other two models, not only with lower AIC, but also with more accurate parameters estimates.

Thus, 4-parameter models are necessary improvements of vitality based survival model for the populations with a large variance in initial vitality.

However, the biology of survival is beyond mathematics of survival, so that selecting the appropriate model to represent a real survival curve is not straightforward and fitting models to data do require some judgment. Intuitively, when the curve has a very flat beginning stage, the 3-parameter model together with Salinger's algorithm is preferred due to simplicity and time efficiency. If the starting stage is steep, this implies that the population's initial variation is significant, and Gaussian or gamma models should be preferred. As a general guideline, AIC is a good quantitative indicator to make decision among models: generally, the model with lowest (most negative) AIC after fitting will be the most appropriate. However, there are some special situations we need to be concerned. Examples are presented below to give some idea of model selection. Data are from previous research on: giant tortoise

(Bourn, 1978), tortoise (Hellgren, 2007), fruit fly (Carey, 1998), turtle (Gibbons, 1982), and bird (Deevey, 1947). First, 3-parameter model and Gaussian model are applied to those data at the same time. If *u* is bigger than 0.28, a good rule of thumb is to consider using the gamma model also. Results are list in Table 1.

The first example is from two giant tortoise researches (Bourn, 1978 and Hellgren, 2000) that we compared the mortality of two kinds of tortoise. Curve fitting to the first species has a very small *u* (0.022377) leading to a preference for 3-parameter model. But, for the second species, 3-parameter model produces a negative estimate for *r*, which contradicts the biologically meaningful hypothesis that the average vitality for a population should decline with time. This is another big advantage for applying 4-parameter model. It is easy to control the range of the parameter space searched with simulated annealing. And because of adding a new parameter, the loss of changing *r* from negative to positive could be compensated by *u* without sacrificing too much goodness of fitting indicated by AIC. Other examples like turtle and lapwing seem exposed to the same issue and are "corrected" by the 4-parameter model. In these examples, the 4-parameter model is preferred with positive r despite the fact that the 3-parameter model provides lower AIC values. Thus, model selection based on their AIC doesn't always hold.

The 3-parameter model is ultimately just a special case of 4-parameter Gaussian model with *u* fixed at zero. Since *u* is a meaningful parameter, it can be argued that it should be retained in any situation. When *u* is small, although the AIC value from 3-

parameter model is lower than that from 4-parameter Gaussian model, the estimated parameters *r*, *s* and *k* are essentially the same, which means 3-parameter model could be replaced by 4-parameter models under most conditions. The main reason we reserve the 3-parameter model is the simplicity and efficiency of the parameter estimation procedure. Also, we may want to compare 4-parameter models with it to check the accuracy of parameter estimation, specifically for small u.

The second example with issue in selecting models is illustrated with the med fly data. It is a nice example showing how the values of *u* influence the AIC but not model selection. Small *u* corresponds with a better fitting for 3-parameter model while big *u* prefers a 4-parameter model based on AIC only. A examining of results from estimation tells that the parameters from 4-parameter Gaussian are almost the same as those from 3-parameter model. Using 4-parameter Gaussian, we do not lose any quality of the fit, but we gain more information with additional parameter *u*. We have displayed the second species of fruit fly of this example in the introduction section to reveal the limitation of 3-parameter model. It is noted that the 4-parameter allows for curvature in early life history where the 3-parameter model is incapable of achieving. It always makes a straight line decline in survival in the early life. The 4-parameter model gives a gradual humped decline: a concave shape in early life. Thus, the amount of early life humping may be an indication of heterogeneity in initial distribution.

It is interesting to look at the last example about the survivorship rate of various birds. The parameters estimated with 4-parameter model are quite different from those estimated with 3-parameter model. I doubt it is because the available data points are too few and the second available survival rate is no bigger than 60% for each curve. However, 4-parameter model seems to behave better in this case with lower AIC value and more important, it doesn't have an artificial flat stage comparing to 3-parameter model. Moreover, this example is chosen not only to exhibit how to select model, but also set as an example of how to compare the mortality of two populations based on vitality model parameters. Take British robin and starling as example, which two experience similar life history. The second population survives better than the first one with a smaller r and k, which could be explained as starling is superior to British Robin both in the loss rate of living capacity and accidental mortality rate. The first population is also more heterogeneous indicating by a larger s and u. Since vitality models provide options to decompose survival into four meaningful parts, it simplexes the system and gives a more efficient way to look at the system.

Based on the simulation results in Appendix C, it could be may argued that, using the gamma model reduces the overall risk of being biased, since it is relatively stable except for a slight overestimation of u when the initial variation is small. I partly agree with these statements, but simplicity and efficiency would be other things to consider. Specifically, it is easier and faster to compute the parameters for the Gaussian model, while calculating gamma model would take much more efforts. Until

a better method is found to work with the gamma model, I would prefer to adopt the Gaussian model first and consider the gamma model when the estimate for *u* is large enough like>0.25.

Summary of Conclusions

Figure 9 shows the fit of survival curves to data. It is hard to distinguish visually between the 3- and 4-parameter models in most cases. But for the fruitflies and birds cases, 4-parameter model is obviously better than the 3-parameter model. However, in some situations 3- and 4-parameter model have very different parameter values, particularly in the case when $r<0$ in the 3-parameter model. Thus, I conclude that in most situation it is better to fit data with the 4-parameter Gaussian model first, and use gamma model only when *u* is relative big (e.g. >0.25). The 3-parameter model may be conducted to check the accuracy. If there is any disagreement, we should generally trust 4-parameter models more than the 3-parameter model.

Table 1: Parameter estimation from various species of animal survival data

	3-para model				4-para Gaussian model				
	r1	S1	k1	AIC	r2	s2	k2	u2	AIC
Bourn(1978),giant tortoise									
Tortoise.giant	0.052	0.103	0.027	-80.1	0.052	0.102	0.028	0.012	-78.3
Tortoise.hermann.f	-0.174	0.608	0.125	-187.7	0.000	0.521	0.087	0.284	-189.9
Carey(1998),drosophila reproduction)									
Fruitfly.f	33.000	2.893	0.000	-112.2	33.013	2.892	0.000	0.001	-110.2
Fruitfly.g	6.286	0.461	2.547	-591.7	6.674	0.008	1.519	0.231	-661.8
Gibbons(1982),turtle									
Turtle	-0.757	0.367	0.256	-134.0	0.058	0.008	0.252	0.024	-132.6
Deevey(1947), agregate									
Blackbird	0.562	0.989	0.055	-74.9	0.002	0.982	0.376	0.259	-78.6
thrush	0.637	0.935	0.057	-65.8	0.000	0.838	0.491	0.269	-68.4
robin.b (British Robin)	0.673	0.743	0.052	-55.7	0.195	0.230	0.694	0.190	-80.0
starling	0.561	0.756	0.110	-62.4	0.160	0.157	0.671	0.010	-74.5
lawping	-1.155	1.047	0.388	-117.8	0.086	0.009	0.425	0.017	-95.5

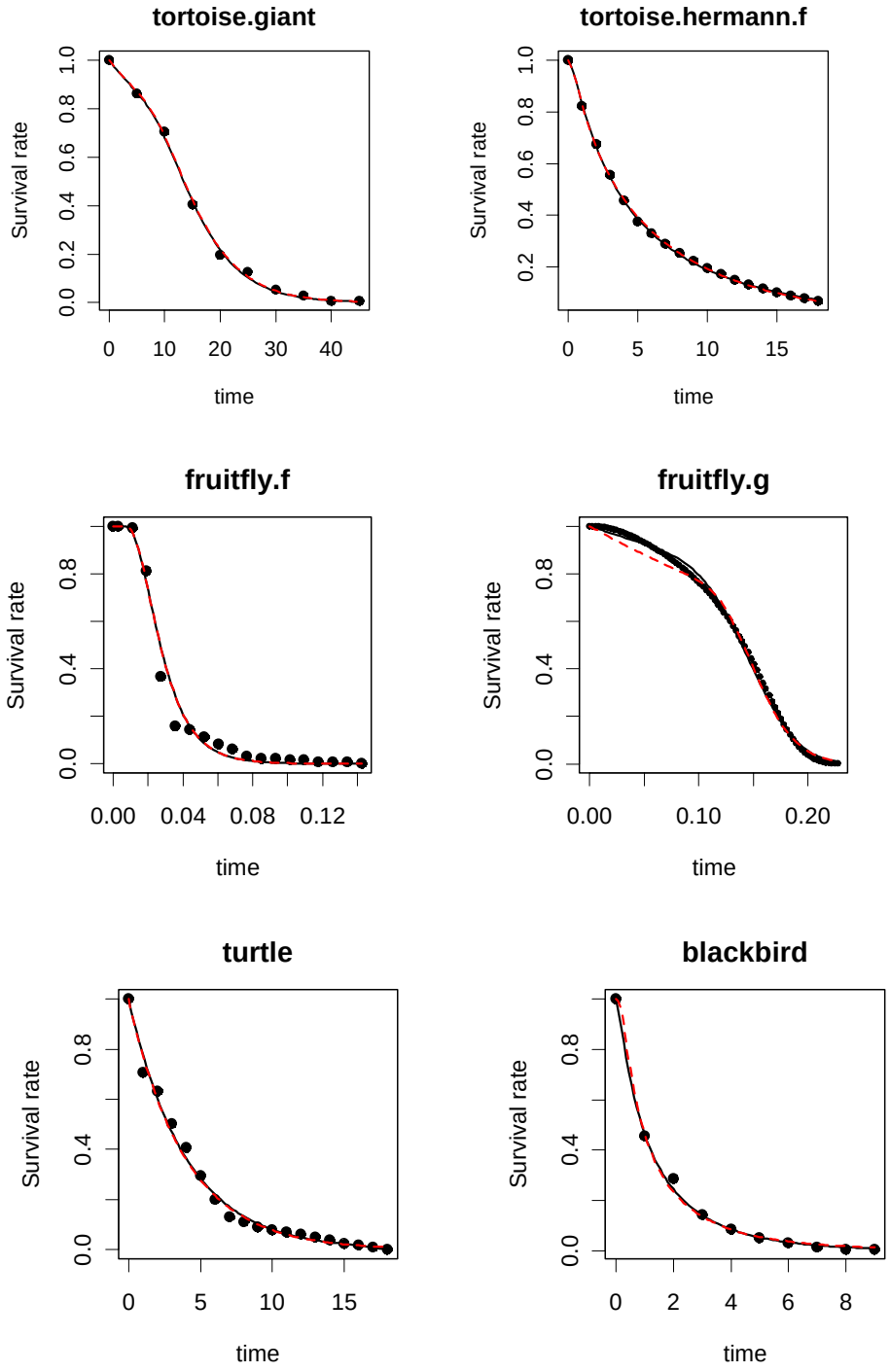

Figure 9: Model fit to survival curves of different animals. X-axis: time (year) and y-axis: survival rate. Solid line: 4-parameter model Gaussian model, dash line: 3-parameter model.

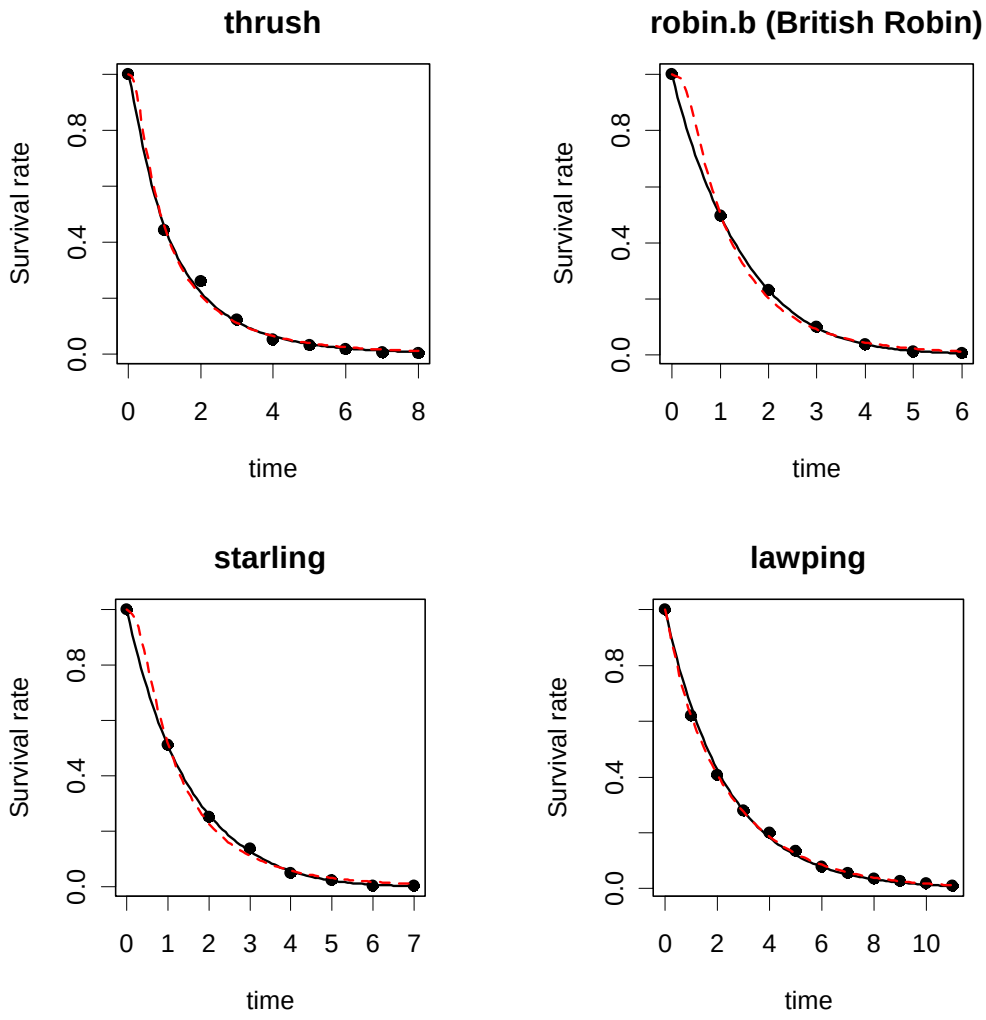

Figure 10: Model fit to survival curves of different animals. X-axis: time (year) and y-axis: survival rate. Solid line: 4-parameter model Gaussian model, dash line: 3-parameter model (cont.).

Chapter III: Application to Human Mortality Data

Demographers have made great effort to understand population survival dynamics of humans. A major focus in these studies has been to discover biological patterns of the life span of individuals (Carnes and Olshansky 1993). Since 1970s, demographers realized the importance of population heterogeneity in estimating life expectancy and rates of aging (Vaupel et al. 1979; Vaupel et al. 1998). A foundation of biodemography, the Gompertz law of mortality (Gompertz 1825), describes mortality rate, u_x, as an exponentially increasing function of age x, such that $u_x = ae^{bx}$ where a and b are intercept and slope constants. However, observations indicate that at old age the mortality rate decelerates, or plateaus, in many populations from flies to humans (Cary et al. 1992; Vapel et al. 1998; Gavrilov and Garilova 2003; Rauser et al. 2006). To reconcile the disconnect between the Gompertz model and observations a number of studies have proposed a demographic heterogeneity characterized by subpopulations with distinct Gompertz coefficients, which produce mortality rate plateaus when the weak cohorts die early and the stronger subpopulations remain (Carey 1997; Service 2000; Carnes and Olshansky 2001; Miyo and Charlesworth 2004; Wu et al. 2006). The view of introducing heterogeneity made models more realistic, helping correct the bias from estimation of life table (Vaupel et al. 1979) and characterize the properties of data from observation. But the ways of representing heterogeneity by those models are inadequate to consider the dynamics producing heterogeneity. Thus, they are unable to display how the population structure changes with heterogeneity.

We apply the vitality model to explore how heterogeneity in vitality may provide an

alternative framework in which to view the complex process in human survival patterns. Therefore, we not only want to fit the survival data, but also try to explain some important features characterizing mortality rate. Due to the abundance of data available in demography, applying the vitality model to human mortality data did reveal something interesting and fundamental patterns that have not been considered previously.

Parameter Estimation

National-level mortality data of Denmark from Human Mortality Database (Wilmoth and Shkolnikov) are used. Data are organized by cohort with birth year from 1835-1895 and life period from age 0 to age 110. For each cohort, we left-truncate life survival curve by every 10 year. For example, 9 survival curves are generated from the cohort with birth year at 1885, corresponding to age ranges 0-110, 10-110, 20-110, 30-110, 40-110, 50-110, 60-110, 70-110, and 80-110 separately. I fit vitality model to each curve respectively. The Gaussian initial model is implemented to the first 7 curves while gamma initial model is applied to the last two since old age population tend to have large variation and are more likely to have a gamma initial distribution. Figure 10 shows the fitting results for cohort with birth year at 1885. Except for the first curve, vitality model fits the data quite well especially for the old ages. I suggest that the failure of fitting early age is because the accidental mortality (i.e. age independent) rate in infants is much higher than the average accidental mortality of adults. Since our model assumes the average accidental mortality is a constant among the age range of fitting curve, it fails to capture this big gap. Possibly, early life mortality could be the result of different r, s and k parameters as well as an initial distribution. Typically, demographic models fit curves like the Gompertz curve to

adult populations and disregard the very-young. Some of the improved models are designed to fit the early age data by making subpopulations characterized with different parameters (Yashin, et al. 2001). Similar method may be adopted with a vitality model, but it is out of the scope of this thesis. However, almost perfect fitting for later ages really indicates much information. Table 2 lists the parameters estimated from vitality model of cohort 1885.

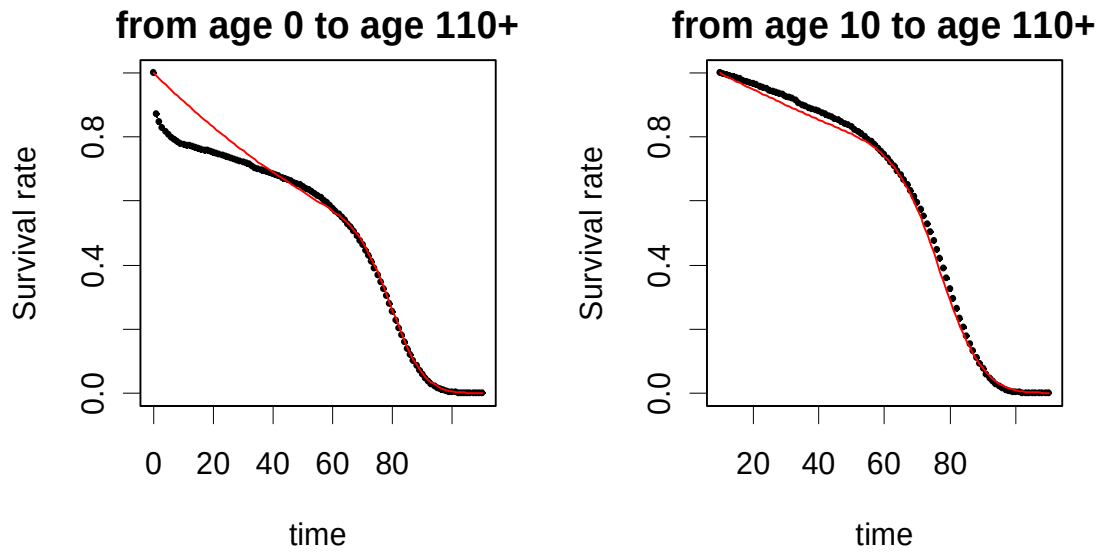

Figure 11: fitting results for truncated survival curves from Danish cohort data with birth year at 1885. The Gaussian was fit for the first 7 curves and the gamma model for the last two oldest curves.

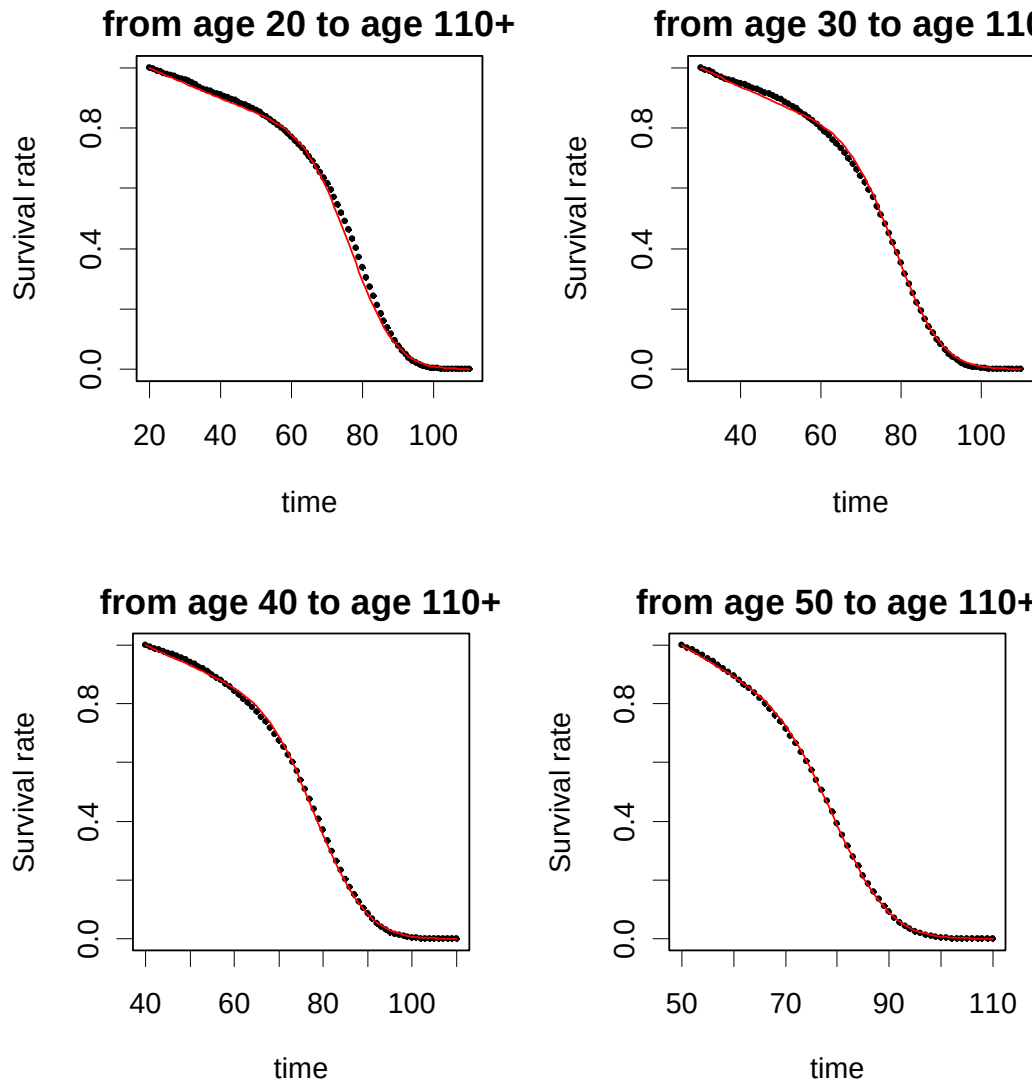

Figure 12: fitting results for truncated survival curves from Danish cohort data with birth year at 1885. The Gaussian was fit for the first 7 curves and the gamma model for the last two oldest curves (cont.).

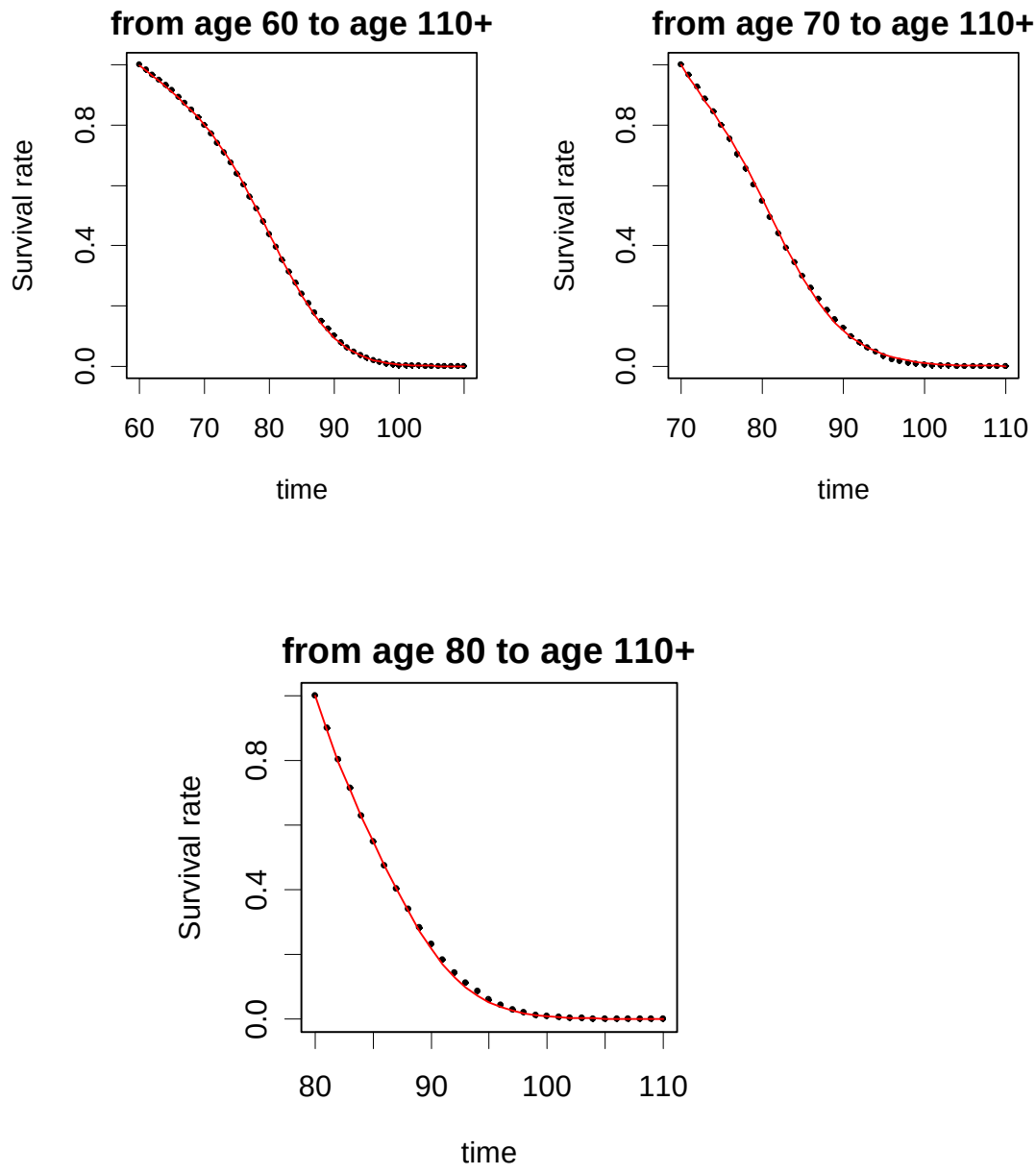

Figure 13: fitting results for truncated survival curves from Danish cohort data with birth year at 1885. The Gaussian was fit for the first 7 curves and the gamma model for the last two oldest curves.

Table 2: parameter estimates for cohort 1885 (standard errors of the estimates are listed in brackets)

age	0-110	10-110	20-110	30-110	40-110	50-110	60-110	70-110	80-110
r	0.012	0.015	0.017	0.020	0.025	0.033	0.044	0.060	0.076
	(6E-6)	(8E-6)	(2E-5)	(2E-5)	(4E-5)	(7E-5)	(1E-4)	(5E-4)	(6E-4)
s	0.003	0.002	0.004	0.003	0.003	0.003	0.020	0.046	0.043
	(2E-4)	(8E-4)	(2E-4)	(4E-4)	(5E-4)	(8E-4)	(9E-4)	(8E-4)	(7E-4)
k	0.010	0.005	0.006	0.006	0.007	0.010	0.018	0.042	0.114
	(5E-5)	(4E-5)	(4E-5)	(5E-5)	(6E-5)	(1E-4)	(2E-4)	(3E-4)	(3E-4)
u	0.098	0.137	0.176	0.193	0.236	0.283	0.317	0.349	0.354
	(1E-4)	(1E-4)	(1E-4)	(2E-4)	(2E-4)	(3E-4)	(5E-4)	(1E-3)	(2E-3)

The Pattern of r

Noticed from the first two plots of Figure 11 that estimated *r* is increased as the starting age goes up and *log(r)* is nearly linearly against age. In vitality model, $r = \rho / \overline{v}$ is the normalized average vitality loss. $\overline{v}$ is the average vitality at beginning time for vitality, while ρ is the absolute average vitality loss, which is proposed (Anderson et al 2008), may represent the average decreasing rate of cell function contributing to accumulated damage of body. According to basic model assumption, ρ is constant across the fitting

range, but ρ might be different as the left truncation age of the data is altered. Under the assumption that the initial vitality is described by a Diric delta function, so all individuals are identical at birth, the average vitality $\overline{v}$ as a function of age (T) is

$$\overline{v}_* = \frac{\int_0^\infty v p_v(v,T)\,dv}{\int_0^\infty p_v(v,T)\,dv} = \frac{\Phi\left(\frac{1-r_*T}{s_*\sqrt{T}}\right) + \exp\left(\frac{2r_*}{s_*^2}\right)\Phi\left(-\frac{1-r_*T}{s_*\sqrt{T}}\right)}{\Phi\left(\frac{1-r_*T}{s_*\sqrt{T}}\right) - \exp\left(\frac{2r_*}{s_*^2}\right)\Phi\left(-\frac{1-r_*T}{s_*\sqrt{T}}\right)} - r_*T \qquad 16)$$

where r_* and s_* are the parameters of a survival curve beginning with point source of vitality (Anderson et. Al. 2008). Here we use r and s estimated from curve starting at age 10 to approximate r_* and s_*, since the initial variation is small at early age groups. Thus, we are capable of estimating $\overline{v}_t$ at each starting age as the average initial value of vitality for each curve. Then ρ_t is recovered following the relationship of $\rho_t = \overline{v}_t \times r_t$. Specifically in this example, t means the starting age and ρ_t is the absolute average rate of vitality loss, which is a constant over the curve starting from age t to age 110. Shown by fig. 11(3), ρ_t is flat at early starting age, but begins dropping around age 60. As ρ_t somehow represents the average rate of senescence, the decline may be a sign of average senescence slowing down at older ages.

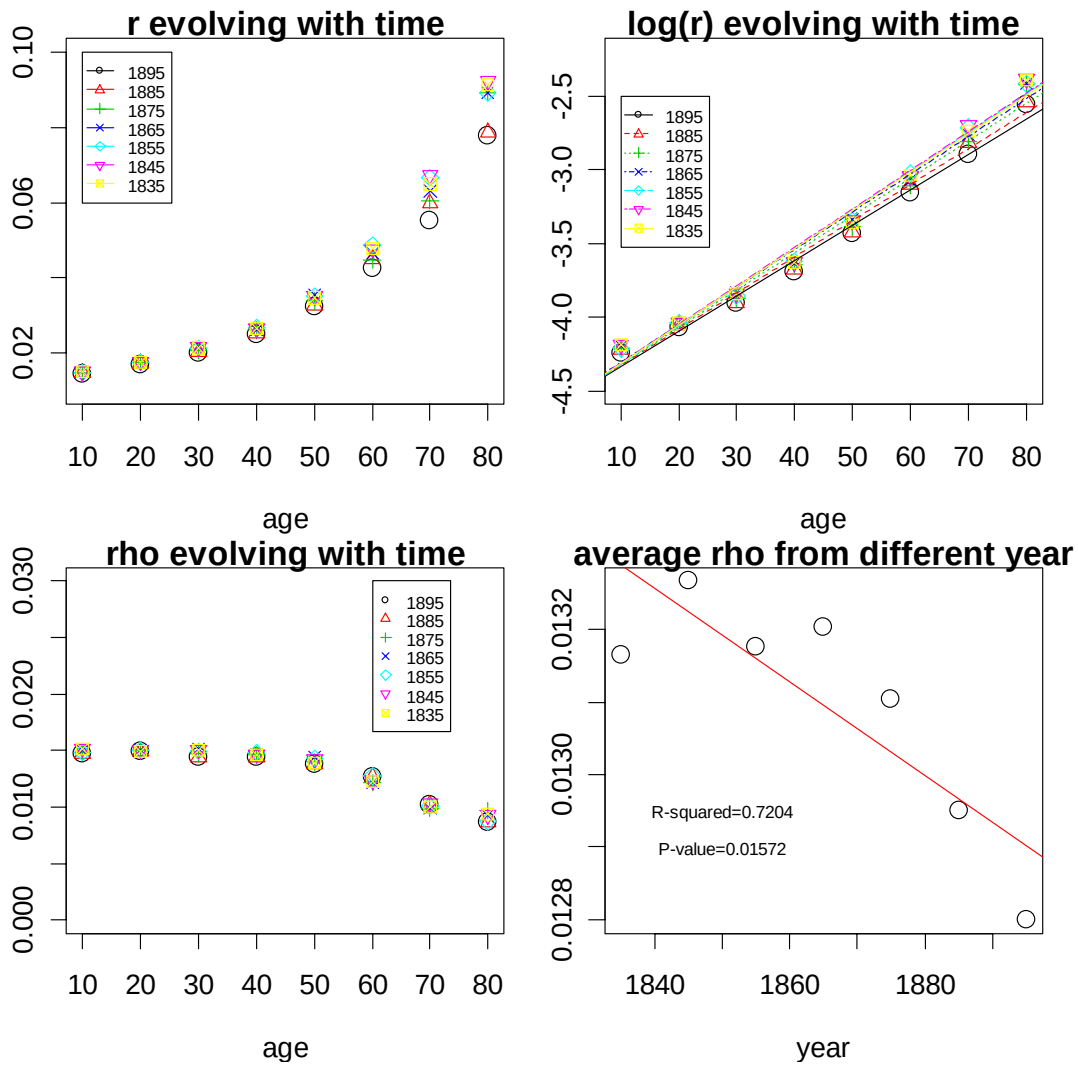

Figure 14: Parameter *r* and estimated ρ from Denmark's human survival data with cohort 1835,1845,1855,1865, 1875, 1885 and 1895. The original and log scale *r* against initial age comparing among cohorts are shown in plot 1 and 2separately. Plot 3 is the absolute parameter ρ changing with starting age, while plot 4 indicates the average ρ vs. cohort years.

The Pattern of u

Similar to *r*, u_t standing for the standard deviation of the initial distribution of vitality in the model is also ascending with the increase of initial age (fig. 12). Using the same

approach, τ_t could be recovered from $\overline{v}_t \times u_t$ which represents the absolute standard deviation of initial vitality. However, the declining trend of τ_t seems contradictive with the trend of u_t (fig. 12). Either u_t or τ_t might be considered as a representation of the biological variation of a population. There is a debate about the age-specific pattern of genetic variation among population. Some drosophila experiments report that the variation was relatively high at early and intermediate ages and then declined at older ages (Promislow et al. 1996, Pletcher et al. 1998), which appears to be favored by the trend of τ_t. But Service (2000) argued that the decline of variation that had been observed in those experiments was an artifact of heterogeneity and the real variation should keep increasing until approach to an asymptotic value. He further stated the reason of this contradiction was the individuals who survive to old ages were not truly representative of their cohorts. Thus, "observations of the surviving population cannot be directly translated into conclusions about the behavior or characteristics of the individuals who made up the original population"(Vaupel and Yashin 1985). Back to our vitality model, remember that the stage of quasistationary distribution mentioned before where the mortality rate is a constant and the distribution of vitality converges to a limiting distribution. Probably, this is not the most appropriate statement. A better way is that when the process reaches its quasistationary distribution, as the dying of individuals from the population, the probability mass of vitality is continuously dropping off, but when we renormalized the probability mass to 1, the distribution stays stable as the quasistationary one. Thus, the real pattern of age-specific variation should behave like *u* that goes up and hits an asymptotical value which is the variation of the limiting distribution of the process

(Aalen and Gjessing 20001). What we can observe in population variation is usually the trend of τ . Intuitively, this disconnection between real variation and observing variation is caused by the shrink of population size which is the same idea of Service (2000) that the available survival population at old ages may be only a part of the truly population. By somehow, we can still catch the real variation in some experiments when death is not significantly occurring. A review of gerontological studies shows that the variability of a majority of biological and cognitive health indicators tends to increase with age. (Nelson et al. 1992) Likewise, a longitudinal study of blood pressure among nearly 4000 men over a 40-year period found increasing variability with increasing age. (Tate et al. 1995) These empirical results on age-related variability are compatible with what we got and even confirm our explanation of the pattern of parameters. Notice that Zens and Peart (2003) have discussed the need of considering hazard functions that account and readjust for the remaining population. But the vitality model does this automatically.

It seems that the features of vitality model itself solves the contradiction between u and τ , and the shape of u is understood. In this paragraph, we'll look in detail how the shape of τ in fig.12 (2) is produced. A simulation is conducted using the similar values of parameters to the human mortality data. The simulation is just like what we did in chapter II that thousands of vitality trajectories are created and we directly calculate the variation of vitality distribution at each time point. This gives the simulation value of τ shown in fig. 13(2). τ increases in the early and intermediate ages but falls down at old ages, which is consistent with the observation in many experiments (Promislow et al. 1996, Pletcher et al. 1998). Comparing fig. 12 (2) with fig.13 (2), τ estimated from real data doesn't capture the early increase trend. One possible explanation is the overestimate of u as well

as τ starting at early ages. Look at fig. 10, the fitting results for truncated survival curves from Danish cohort data with birth year at 1885. It seems like the model did not fit data that well for the first four plots (starting at age 0, 10, 20, 30.) comparing to the last five. The fitting curves are a little bit under the real curves, which could be a sign of overestimate. Check fig. 5 in chapter I: the bigger the u is, the steeper the curve is at the beginning. And u is quite sensitive for the bias; therefore a little deviation will cause a significant change of u. That is why there is not an early increase of τ of human data.

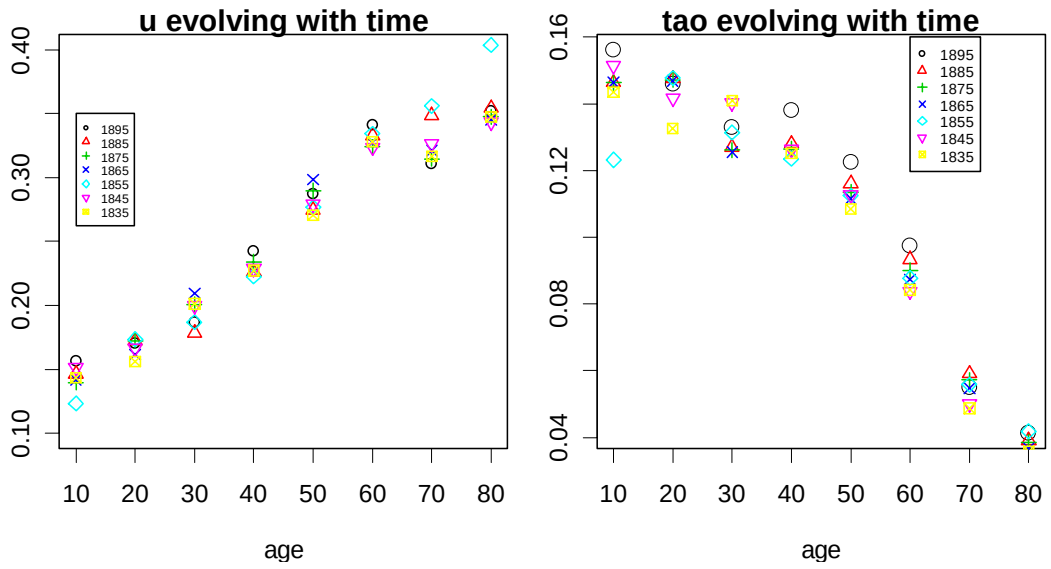

Figure 15: Parameter u and τ estimated from Denmark's human survival data with cohort 1835,1845,1855,1865, 1875, 1885 and 1895.

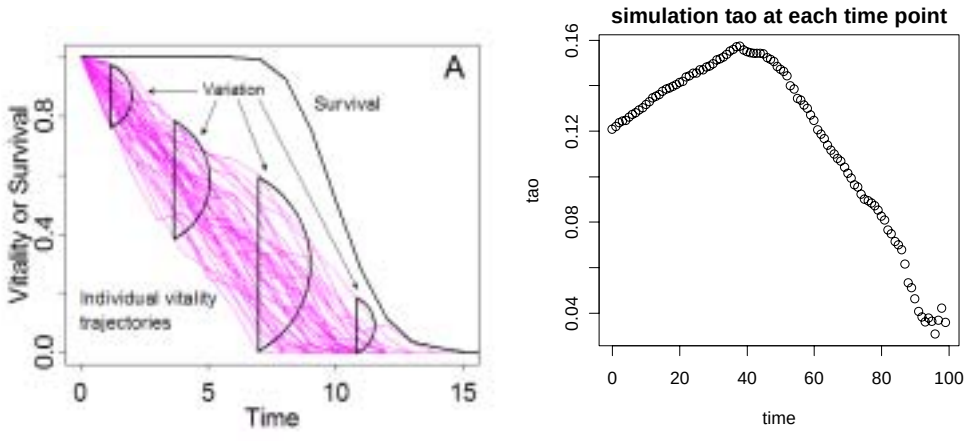

Figure 16: calculation τ from simulation. The first plot shows directly how we calculate τ at each time point from vitality trajectories. The second plot is the simulation results.

The Pattern of s and k

The pattern of *s* and *k* is a little different. Both s and k are relatively stable if starting at an early age, but suddenly increase to a high level at older beginning ages. For $\sigma_t = \overline{v}_t \times s_t$ the absolute magnitude of the stochastic term, there has a slowly ascending trend at old ages as shown in fig. 14 (2). For *k*, indicating the accidental mortality rate, a reviewing of U.S. monthly vital statistics report, advance report of final mortality statistics over a period of 1977 to 1995 clearly shows that the death rate caused by accidents, homicide and suicide has a dramatic increase around age 75 after following a flat beginning, which is almost perfectly implied by this vitality model. Reports from year 1979 and 1995 are listed in Table 3. Mortality is expressed as the number of death every 100,000 people.

Table 3: Monthly Vital Statistics Report, Report of Final Mortality Statistics, 1995
Accidental mortality by age (every 100,000 people)

age	0-1	1-4	5-14	15-24	25-34	35-44	45-54	55-64	65-74	75-84	85+
1979	31.5	26.5	16.1	62.6	45.7	38.4	39.4	43.5	58.8	117.8	276
1995	20.5	14.5	9.3	38.5	32.9	33.5	29.8	31.9	44.8	98.4	268.2

One common characteristic among parameters is a significant altering of structure happening after age 60. There might be some fundamental change pertaining to either the process or the organism function for old population, which have something to do with the hypothesized mortality plateau. As we mentioned before, the vitality distribution converges to its quasistationary distribution at old ages. This has been proved to be a natural way that leads to mortality plateaus by the structure of Winner process itself. We'll further discuss it later.

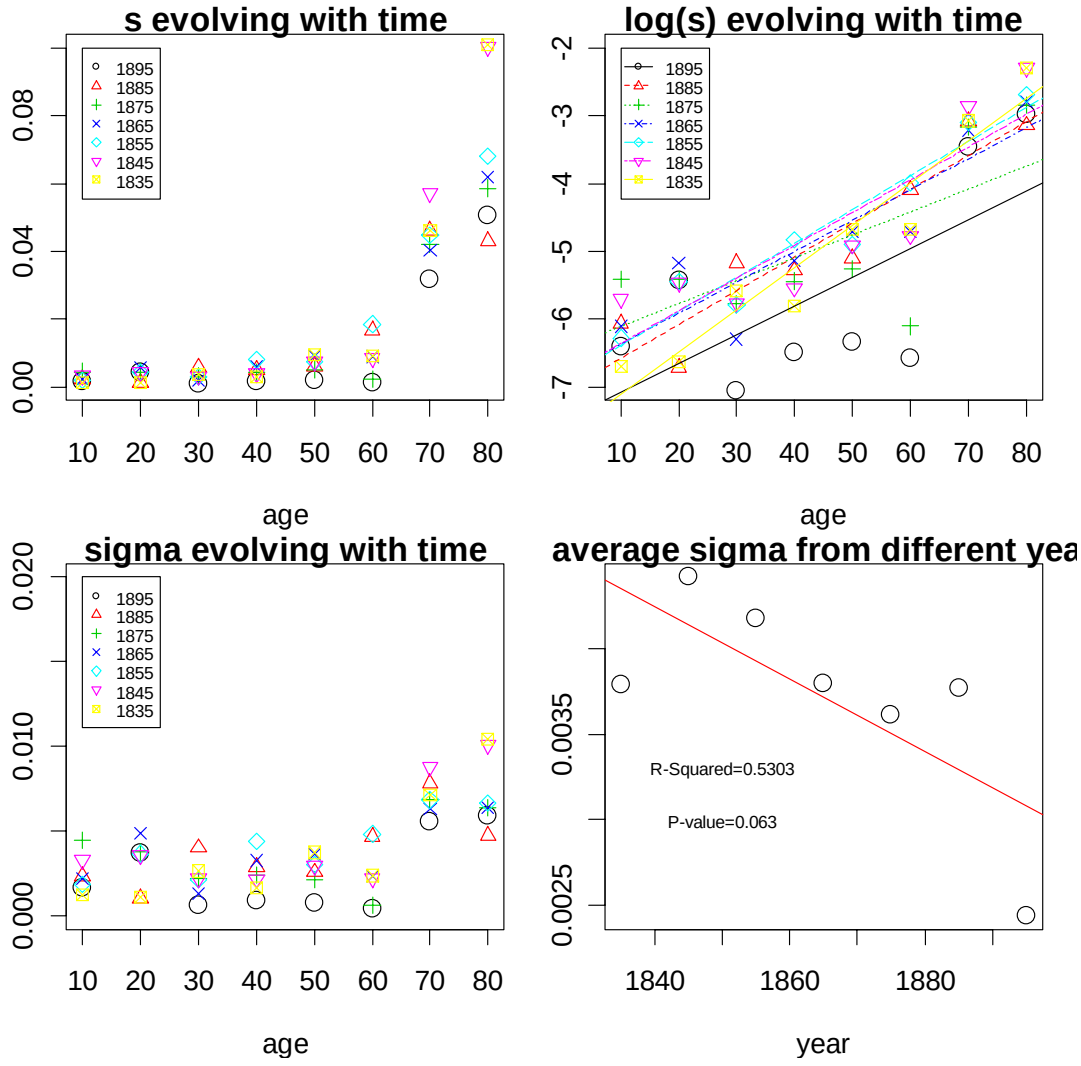

Figure 17: Parameter estimation from Denmark's human survival data with cohort 1835,1845,1855,1865, 1875, 1885 and 1895. The original and log scale s and *k* against initial age comparing among cohorts are shown in plot 1, 2, 5 and 6 separately. Plot 3 is the absolute parameter σ changing with starting age, while plot 4 indicates the average σ vs. cohort years. Plot 7 describes the trend of *k* as the increasing of cohort years. Each line is fixed at a starting age.

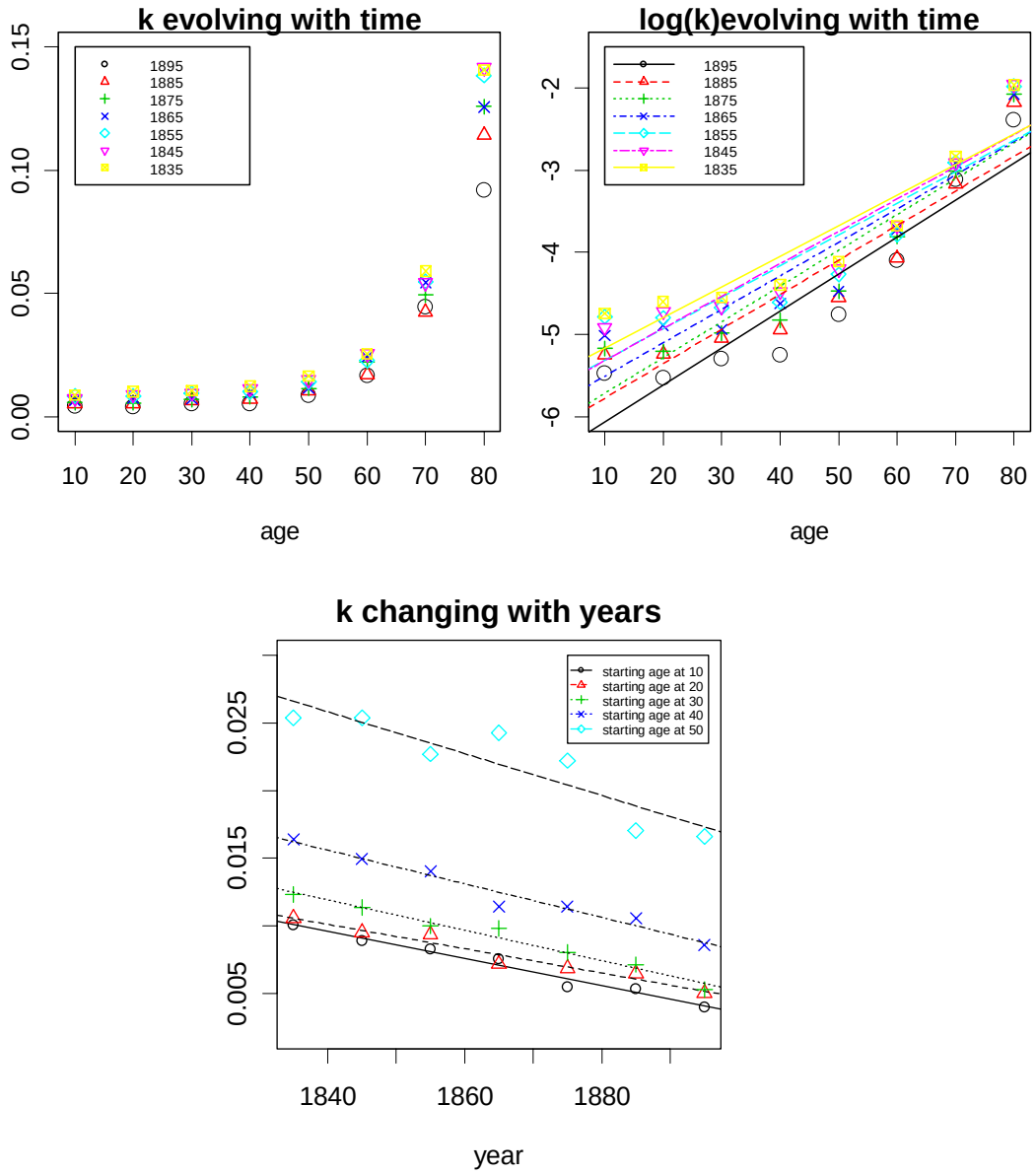

Figure 18: Parameter estimation from Denmark's human survival data with cohort 1835,1845,1855,1865, 1875, 1885 and 1895. The original and log scale s and *k* against initial age comparing among cohorts are shown in plot 1, 2, 5 and 6 separately. Plot 3 is the absolute parameter σ changing with starting age, while plot 4 indicates the average σ vs. cohort years. Plot 7 describes the trend of *k* as the increasing of cohort years. Each line is fixed at a starting age (cont.).

Comparison across Cohorts

Almost the same patterns of estimated parameters have been observed from the data of cohort 1835, 1845, 1855, 1865, 1875 and 1895. Comparing parameters across cohort years will also reveal something interesting. Fig. 11, 12 and 14 shows parameters estimated from truncated survival curves of different cohort years. In Fig. 11 (2), the lines of *log(r)* are well arranged from top to bottom corresponding to cohort from year 1835 to 1895, and the differences of *log(r)* among cohorts are more significant for older ages than younger ages. While in fig. 11 (4), the average ρ of each cohort are plotted against cohort years. A linear descent is strongly suggested by a high R-squared and low p-value. Since r and ρ mainly characterize the normalized and absolute decline rate of organism's living ability respectively, both these plots imply human's survival capability has been significantly improved through years, especially for old ages.

Comparing *k* starting at the same age across cohorts also displays the similar trend that the accidental mortality is declined year by year, which is also consistent with table 4. Fig.14 (7) gives a distinct way to view this trend by showing *k* declines with cohort year for fixed starting ages. Looking at the average σ against cohort years in fig.14 (4), there is a decreasing trend but is not significant suggested by a p-value equaling 0.063. Because parameter τ and normalized u mainly determine the heterogeneity of a population, as shown by fig. 12(1) and (2), no obvious tendency among cohorts for τ and *u* demonstrates that the variance among population is not significantly decided by year.

However, ρ, r together with k are good enough to indicate the survival improvement which has been confirmed by many demographic studies (Yashin, et al. 2001).

In this section, we apply vitality model to fit human survival data, which incorporates parameters directly related to qualitative features such as capacity of living, age-specific pattern of variation among population and accidental mortality. The quantitative analysis shows that the observed trends in human survival can be well explained in terms of the pattern of parameters estimated from vitality model.

Mortality Plateau

One of the most interesting problems in demographical studies is related to mortality plateau which is believed to be critical for explaining the dynamics of senescence. Mortality plateau, as being defined several times previously, is one fundamental problem that the supposedly tenets of ageing, namely the exponential growth of mortality rates proposed by Gompertz (1825), may fail to describe the behavior of observed populations adequately (Weitz and Evans 2001). More specifically, studies using populations or "cohorts" of different animals and humans demonstrate that mortality rates tend to level off and even decease at later stages of life, known as mortality plateaus (Carey et al. 1992; Vaupel et al. 1994, 1998). There are at least two possible explanations for this phenomenon: the heterogeneity hypothesis and the individual-risk hypothesis (Khazaeli et al. 1995). According to the heterogeneity hypothesis, the deceleration is a statistical effect of selection through the attrition of mortality. Because the more frail tend to die at younger ages, survivors to older ages tend to have favorable health endowments and healthy lifestyle. For the individual-risk hypothesis, the age-related increase of mortality

risk for individuals slows down at older ages, which leads to the decline of mortality. Since the vitality model is a simple representation of the complex system and the essential process of ageing and death, the most attractive application would be having something to do with mortality plateau.

First, in some degree, the vitality model does favor the first explanation that heterogeneity among population naturally shapes the survival curve as well as the mortality rate plateaus. The way we represent heterogeneity automatically allows some individuals die early and some survive longer. Early as 2001, Weitz and Fraser have successfully shown the mathematical fundamental of producing mortality plateaus by Winner process based model. In their paper, they proposed a similar model to Anderson's 3-parameter model, only didn't consider accidental mortality. Without applying to any real data, they expressed the hazard rate analytically and displayed that the mortality plateau was physically achieved under different conditions of parameters. Certainly, we could conduct similar analysis and finally end up with the similar results. The new hazard rate of our 4-parameter model would be the similar expression as Weitz and Evans' only plus a constant accidental mortality k, which would not change the shape of hazard rate. Here, the important point is that our vitality model creates an approach to exhibit the mechanism of heterogeneity evolving through ages that could cause a mortality plateau. Secondly, let's look at our process in a deeper way through quasistationary distribution. The stage that the hazard rate is stabilized shown by Weitz and Fraser (2001) is the time the vitality distribution reaches its quasistationary distribution, the time the shape of the probability mass is stable, and the time the level of distribution sinks proportionately at

every location. Then, “the mortality rate, of course, will also approach the mortality rate averaged over this distribution. In other word, the mortality rate stops increasing, not because we have selected out the exceptional subset of the population, but because the condition of the survivors is reflective of their being survivors, even though they started out the same as everyone else.” (Steinsaltz and Evans 2003). Thus, although we adapt an approach of heterogeneity to explain mortality plateau, our way is a little different with the heterogeneity hypothesis proposed before. We neither characterize the variation between populations or select population as time went through. Instead, we only model the heterogeneity within a population and show how it evolves with time. It turns out the mortality plateau will naturally achieve under the way we represent heterogeneity. Finally, besides considering model structure only, applying model to real human survival data suggests something more. Look at the Fig. 11 (3) that the absolute rate of vitality loss ρ against starting ages. A decline happens around age 60 among all the cohorts. As stated above, the drop of ρ is a sign of deceleration of average mortality as well as the average rate of senescence. Purely following the parameter estimation from data, mortality plateau presents itself. However, the explanation for the decline of average rate of vitality loss is not able to recognize one hypothesis from the other. That is both hypotheses could conduct the decreasing of ρ. Our heterogeneity hypothesis assumes that the achievement of quasistationary distribution brings down the average loss rate of vitality at old ages, while individual-risk hypothesis supposes the functional senescence slowing down for each individual contributes to a total decline. Technically, those two hypotheses do not conflict with each other at all. Although the structure of vitality model supports the heterogeneity hypothesis, it does not exclude the second hypothesis. There is

a possibility that the combination of those two hypotheses forces the formation of mortality plateau.

Mortality plateau is still a mystery; however our vitality model makes a good progress to explain it. At least, it provides a way to measure the possible hypotheses.

Discussion

Summary of model

In this thesis, I propose new extensions to the vitality model developed by Anderson (1992, 2000) that add several components to characterize the initial variation of a population. The original vitality model allows heterogeneity within the population as it evolves with age but assumes that the population is homogeneous at the beginning of the survival curve. However, the initial differences among individuals are also important that relate to vital properties of population including inborn genetic heterogeneity and current status of variation that determines the population based mortality in future. Because of being able to represent this initial variance, it allows us to divide a population's life history into distinct stages, where each stage can be independent of its past states, since the beginning status of each stage has been parameterized by u. In another sense, the initial components u also contain the information of former status and could be a summary of heterogeneity evolving with time previous to observing time. Thus, introducing initial distribution into vitality model is not only a matter of modeling but

meaningfully helps to better understand the mechanism of how heterogeneity shapes a population's survival curve.

Here we naturally chose two kinds of initial distribution: Gaussian and gamma, as revealed by the hidden properties of the model itself. Also, in a more general sense, Gaussian is the most common distribution for assembling individuals. And the distribution of vitality tends to stabilize into a gamma distribution pointed by Aalen et al. (2001). The model has successfully implemented Gaussian and gamma functions as the representation of vitality distribution at the beginning of stages. However, it has been shown by Aalen (2001) that if the variation is big enough, vitality will reach a quasistationary distribution. I did not model the transition between Gaussian and gamma to quansistationary distribution, and more important, discuss how the initial distribution will affect the shape quasistationary distribution.

Fitting algorithm

As stated in this thesis, simulated annealing has been used as the mainly algorithm to estimate those parameters. Simulated annealing, as one of those optimization methods that allows jump out of the local optimal values, seems to work well for the vitality model. But the biggest problem for this approach is about timing. Since simulated annealing is a search based method, it is inevitably time consuming. Usually, using a conventional laptop computer, it takes 15 minutes to get a result from a Gaussian initial model comparing to a Newton-Ralphson related method that only uses 5 seconds. For gamma initial model, it is even worse and could take as long as 1 day for one

convergence due to the numerical integral. The ideal algorithm should be like Sailinger's approach, having some restrictions on initial parameter estimation that would increase the speed a lot, but further work is still needed to explore it.

Another thing need to be noticed is the choice of algorithm parameters that control the search process, like the value of initial temperature and the proportion of temperature reduction at each round. It is quite possible that if those parameters are not carefully chosen, the algorithm doesn't guarantee to converge to the right answer. Unfortunately, there is no explicit form to follow and the algorithm parameters may vary as the optimization function changes. Therefore, we can only pick up those values by experiment.

Application to human survival data

The successful application of vitality model to demographic data has explained some important features characterizing survival dynamics in human population, such as the age pattern of survival improvement. Of course, we could do something more using vitality model. If there are enough data available, we are able to comparing survival situation across country, sex, race and et al. based on their vitality parameters.

The most attractive application would be related to the explanation of mortality rate plateaus. We have shown somehow, both the model structure and data exploring will naturally lead to a mortality plateau. Although this model demonstrates why an aging

process should exhibit mortality plateaus, it does not claim to uncover the fundamental causes of aging.

However, the way we use vitality model prove that it could be far more than fitting to data, but a simple way to represent the complex system and reveal the essential process of aging and death.

Further application and final thoughts

It has been noted numerous times that the reason we want to introduce vitality model is to find something fundamental in survival mechanism among different species of animals including humans. This model is in many ways an ideal construct. It subsumes various mechanisms into a single measure of vitality that leads the natural question of how the vitality parameters are correlated with body size, environmental conditions and even genetic differences, if at all. One application of this model is to relate environmental effects or outer treatments to survival through vitality parameters. That is looking at how the external forces change vitality parameters that finally shape the survival curve. Anderson (2000, 2008) has done excellent jobs on discussing those relationships. However, we still need more data both laboratory and natural to complete this system including considering initial distribution into model.

A considerable number of literatures support the hypothesis that gradual cumulative physiological degradation, such as oxidative damage at the cellular level results in organism ageing and eventual catastrophic collapse leading to death. If the concept of

vitality is valid, the process occurs in a similar manner can be linked to a cellular measurement. Therefore, the advanced application could come down to a level of cell and even gene expression.

In another view, as we discussed above, the heterogeneity causing mortality plateaus reveal the idea that the condition of the survivors is reflective of their being survivors. This is somehow a sense of natural selection. If we could further explore how the vitality relates to natural selection thus leading to evolution, this model would have great value. Thus, we believe, although great effort is still needed to consummate our vitality model, it has perspective future both in micro and macro application.

References

Aalen, O. O., and H. K. Gjessing, (2001). Understanding the shape of the hazard rate: a process point of view. Statistical Sciences 16:1-22.

Aars, J., and R. A. Ims. 2002. Intrinsic and climate determinants of population demography: the winter dynamics of tundra voles. Ecology 83:3449-3456.

Anderson, J. J. 1992. A vitality-based stochastic model for organisms survival, in Individual-Based Models and Approaches in Ecology: Populations, Communities and Ecosystems, eds. DeAngelis, D.L. and Gross, L.J. (Chapman & Hall, New York), pp. 256-277.

Anderson, J. J. 2000. A vitality-based model relating stressors and environmental properties to organism survival. Ecological Monographs 70:445-470.

Anderson, J. J., E. Gurarie, and R. W. Zabel. 2005. Mean free-path length theory of predator-prey interactions: application to juvenile salmon migration. Ecological Modeling 186:196-211.

Anderson, J. J., Molly C. Gildea, Drew W. Williams and Ting Li. 2007. Linking growth, survival and heterogeneity through stochastic vitality. The American Naturalist Vol.171, No.1 E-article.

Bourn, D., M.Coc. 1978. The size, structure and distribution of the Giant tortoise population of Aldabra. Philosophical Transaction of the Royal Society of London. Series B, Biological Science, Vol. 282, No. 988, 139-175.

Boyce, M.S., C.V. Harida, T.C.Lee, and the NACEAS Stochastic Demography Working Group.2006 Trend Ecology and Evolution 21:142-148.

Burnham, K. P. and D. R. Anderson. 2002. Model selection and multimodel inferences: a practical information-theoretic approach. Springer-Verlag New York.

Carey, J.R. 1997. What demographers can learn from fruit fly actuarial models and biology. Demography 34:17-30.

Carey, J.R., P. Liedo, D. Orozco and J. Vaupel. 1992. Slowing of mortality rates at older ages in large medfly cohorts. Science 258, 457-461

Carey, J. P.Liedo, H.-G. Müller, J.-L. Wang and J.W. Vaupel. 1998. A simple graphical technique for displaying individual fertility data and cohort survival: case study of 1000 Mediterranean Fruit Fly females. Functional Ecology 1998, 12, 359-363.

Carnes, B.A., and , S. J. Olshansky. 1993. Evolutionary perspectives on human senescence. Population and Development Review 19:793-806.

Carnes, B.A., and S. J. Olshansky. 2001. Heterogeneity and its biodemographic implications of longevity and mortality. Experimetal Gerontology 36:419-430.

Carter, Jacoby, Azmy S. Ackleh, Billy P. Leonard, Haibin Wang. 1999. Giant panda (*Ailuropoda melanoleuca*) population dynamics and bamboo (*subfamily Bambusoideae*) life history: a structured population approach to examining carrying capacity when the prey are semelparous. Ecological Modeling 123:207-223.

Chhikara, R. S., and J. L. Folks. 1989. The inverse Gaussian distribution: theory, methodology, and applications. M. Dekker, New York.

Corana, A., M. Marchesi, C. Martini, and S. Ridella. 1987. Minimizing Multimodal Functions of Continuous Variables with the "Simulated Annealing" Algorithm. ACM Transactions on Mathematical Software, Vol.13, No.3, Pages 262-280.

Deevey, Edward S. Jr. 1947. Life tables for natural populations of animals. The Quarterly Review of Biology, Volume 22, Issue 4, 283-314.

Engen, S., R. Lande, and B. –E. Sæther. 2003. Demographic stochasticity and allee effects in populations with two sexes. Ecology 84:2378-2386.

Fox, G. A., and B. E. Kendall. 2002. Demographic stochasticity and the variance reduction effect. Ecology 83:1928–1934.

Gibbons, J. Whifield and Raymod D. Scmlitsch. 1982. Survivorship and Longevity of a Long-Lived vertebrate species: how long do turtles live? The Journal of Animal Ecology, Vol. 51, No. 2, 523-527.

Gavrilov, L. A., and N. S. Gavrilova. 2003. The quest for a general theory of aging longevity. Science of Aging and knowledge environment. SAGE KE sageke.science.org/cgi/content/ful/sageke;2003/28/re5

Gompertz, B. 1825. On the nature of the function expressive of the law of human mortality and on a new mode determining life contingencies. Philos. Trans. R. Soc. London 115,513-525.

Gurarie, Eli, 2007. Incorporating population-level heterogeneity into analysis of animal dispersal with applications to travel times of migrating juvenile salmon. (Manuscript)

Hellgren, Eric C., Richard T. Kazmaier, Donald C. Ruthven III, David R. Synatzske. Variation in Tortoise life History: Demography of Gopherus berlandieri.

Kendall, M., Stuart, A., 1997. The advanced theory of statistics, 4th ed., vol. 2. MacMillan, New York, USA.

Khazaeli, A.A., L. Xiu and J, W, Curtsinger. 1995. Stress Experimets as a Means of Investigating Age-Specific Mortality in Drosophila melongaster. Experimental Gerontology 30:177-84.

Kirkpatrick, S., Gelatt, C.D., JR., and Vecchi, M.P. 1983. Optimization by simulated annealing. Science 220, 4598, 671-680.

Lande, R., S. Engen, and B. –E. Sæther, and T. Coulson. 2006. Estimating density dependence from time series of population age structure. American Naturalist 168:76-87.

Letcher B, H. J. A. Rice, L. B. Crowder, and F, P. Binkowski. 1996. Size-dependent effects of continuous and intermittent feeding on starvation time and mass loss in starving yellow perch larvae and juveniles. Transactions of the American Fisheries Society 125:14-26.

May, R. M. 1973. Stability and complexity in model ecosystems. Princeton, Princeton University Press.

Metropolis, N., Rosenbluth, A.,Rosenbluth, M.,Teller, A., and Teller, E. 1953. Equation of state calculations by fast computing machines. J. Chem. Phys. 21, 1087-1090.

Miyo, T., and B. Charlesworth. 2004. Age-specific mortality rates of reproduction and non-reproducing males of *Drosophila melanogaster*. Proceedings of the Royal Society B 271:2571-2522.

Nelson, E. and Dannefer, D. (1992) Gerontology 32, 17-23

Pletcher, S. D., D. Houle, and J. W. Curtsinger. 1998. Age-specific properties of spontaneous mutations affecting mortality in *Drosophila melanogaster*. Genetics 148:287-303.

Promislow, D. E. L., M. Tatar, A. A. Khazaeli, and J. W. Curtsinger. 1996. Age-specific patterns of genetic variance in *Drosophila melanogaster*. I. Mortality. Genetics 143:839-848.

Rauser, C.L., L. D. Mueller, and M. R. Rose. 2006. The evolution of late life. Ageing Research Reviews 5:14-32.

Salinger, D. H., J. J. Anderson, and O. S. Hamel.2003. A Parameter estimation routine for the vitality-based survival model. Ecological Modeling 166:287-294.

Service, P. M. 2000. Heterogeneity in individual mortality risk and its importance for evolutionary studies of senescence. American Naturalist 156:1-13.

Steinsaltz, D., and S. N. Evans. 2004. Markov mortality models: implications of quasistationarity and varying initial distributions. Theoretical Population Biology 65:319-337.

Steinsaltz, D. 2005. Re-evaluating a test of the heterogeneity explanation for mortality plateaus. Experimental Gerontology 40:101–113.

Steinsaltz, D. and S. N. Evans. 2007. Quasistationary distributions for one dimensional diffusions with killing. Transactions of the American Mathematical Society: vol 359, no.3, pages 1285-1324

S. Weitz, Joshua and B. Fraser Hunter. 2001. Explaining mortality rate plateaus. PNAS vol. 98 no. 26.

Tate, R., Manfreda, J., Krahn, A., and Cuddy, T. 1995. Am. J. Epidemiol. 142, 946-954

Vaupel, J.W., Manton, and K.G., Stallard, E., 1979. The impact of heterogeneity in individual frailty on the dynamics of mortality. Demography 16:439–454.

Vaupel, J. W., and A. I. Yashin. 1985. Heterogeneity's ruses: some surprising effects of selection on population dynamics. American Statistician 39:176-185.

Vaupel, J., Johnson, T. & Lithgow, G. 1994. Rates and mortality in population of Caenorhabditis elegans. Science 266, 826-828.

Vaupel, J. W., J. R. Carey, K. Christensen, T. E. Johnson, A. I. Yashin, N. V. Holm, I. A. Iachine, V. Kannisto, A. A. Khazaeli, P. Liedo, V. D. Longo, Y. Zeng, K. G. Manton, and, J. W. Curtsinger. 1998. Biodemographic trajectories of longevity. Science 280:855–860.

Weitz, J. S., and H. B. Fraser. 2001. Explaining mortality rate plateaus. Proceedings of the National Academy of Sciences 98:15383–15386.

Wilmoth, John R. and Vladimir Shkolnikov. The Human Mortality Database. http://www.mortality.org/

Wu, D., S.L. Rea, A. I. Yashin, and T. E. Johnson.2006. Visualizing hidden heterogeneity in the isogenic populations of *C. elegans*. Experimental Gerontology 41:261-270.

Yashin, Anatoli I., S. V. Ukraintseva, G. De Benedictis, Vladimir N. Anisimov, Alexander A. Butov, Konstantin Arbeev, D. A. Jdanov, S. I. Boiko, A. S. Begun, M. Bonafe and C. Franceschi. 2001. Have the oldest adults ever been frail in the past? A hypothesis that explains modern trends in survival. The journals of Gerontology: Biological sciences. Vol. 56A. No.10. B432-B442.

Zens, M. S. and D. R. Peart. 2003. Dealing with death data: individual hazards, mortality and bias. Trends in Ecology and Evolution 18:366–373.

Appendix A: Background on Vitality Model

Traditionally, differential equations are widely used to model survive rate. However, this method has its biggest shortcoming that it ignores the nature heterogeneity among population including the initial birth variances and the differences involving further over time. Heterogeneity is one of the most important properties for a population which is believed to be significant to issues of population regulation, extinction and evolution. Several ways have been developed to deal with heterogeneity such as Individual Based Model that tracks population traits at individual level. But even significant progress has been made in developing IBMs, they still lack a standardized approach for representing heterogeneity. A totally new vitality model for fitting survival cures was initially published in a paper by Anderson in 2000. The vitality model for survival is a method by which to characterize the complex interactions between external and internal processes of a given organism. It has two components, one based on past history and related to vitality, and the other one independent of past history and representing accidental mortality.

For vitality-dependent part, each organism within a population is born with a certain amount of vitality v_0. Vitality, denoting the remaining survival capacity of an organism, is a real positive number that evolves with age as a continuous Wiener process. The rate of vitality loss is described by Equation (1)

$$dv/dt = -\rho + \sigma\varepsilon_t \qquad (1)$$

where ρ and σ are the magnitudes of the deterministic (drift) and stochastic (spread) rates of change of vitality, t is age, and ε_t is a white noise process that spreads the distribution. When an organism's vitality reaches zero it dies.

Since the value of the initial vitality of any organism is an unknown quantity, it makes sense to normalize the vitality and parameters ρ and σ by the initial vitality v_0.

$$v = v/v_0 \quad r = \rho/v_0 \quad s = \sigma/v_0 \qquad (2)$$

This creates two new parameters r and s, the normalized rate of vitality drift and the normalized rate of spread.

At a given time t, the probability of a vitality v is defined by equation 3) given the initial vitality v_0. This equation requires all the members of the population have the same initial vitality, describing by a Dirac delta function $\delta(v - v_0)$.

$$p_v(v,t|v_0,0) = \frac{1}{s\sqrt{2\pi t}}\left[\exp\left(-\frac{(v-1+rt)^2}{2ts^2}\right) - \exp\left(-\frac{(v+1+rt)^2}{2ts^2} + \frac{2r}{s^2}\right)\right] \qquad (3)$$

Integrating equation (3) over the allowable range of vitality(0, ∞) gives the probability of survival based on vitality.

For vitality-invariant part, the probability of survival dues to accidental mortality is a Poisson process and defined in equation 4).

$$P_a(t) = e^{-kt} \qquad (4)$$

The probability of survival for a population is the product of the probability of survival based on vitality and the probability of survival due to accidental mortality. The explicit formula is shown in equation 5)

$$l(t) = P_v(t)P_a(t) = \left(\Phi\left(\frac{1}{s\sqrt{t}}(1-rt)\right) - \exp\left(\frac{2r}{s^2}\right)\Phi\left(-\frac{1}{s\sqrt{t}}(1+rt)\right)\right)e^{-kt} \qquad (5)$$

Appendix B: the shape of gamma distribution with restriction mean=1

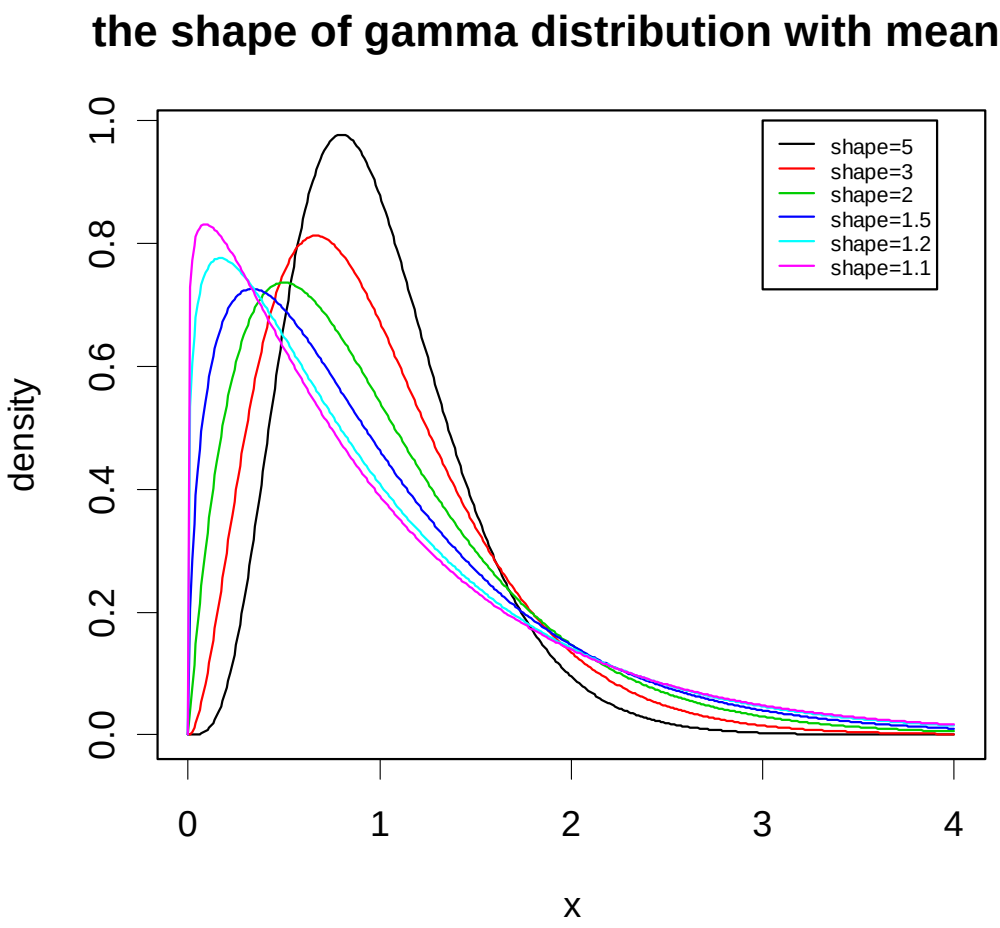

Appendix C: Table for simulation results (standard errors in parentheses)

		r	s	k	u	AIC
Simulation 1 Gaussian	actual para	0.050	0.100	0.005	0.050	NA
	3-para	0.047 (0.001)	0.097 (0.004)	0.005 (0.001)	NA	-503.5
	4-para Gaussian	0.047 (0.001)	0.097 (0.003)	0.005 (0.001)	0.049 (0.002)	-499.4
	4-para gamma	0.046 (0.001)	0.090 (0.003)	0.005 (0.001)	0.141 (0.002)	-416.7
Simulation 2 Gaussian	actual para	0.050	0.100	0.005	0.100	NA
	3-para	0.047 (0.001)	0.097 (0.003)	0.006 (0.001)	NA	-498.3
	4-para Gaussian	0.048 (0.001)	0.094 (0.003)	0.006 (0.001)	0.109 (0.003)	-500.8
	4-para gamma	0.049 (0.001)	0.078 (0.004)	0.003 (0.001)	0.262 (0.003)	-479.6
Simulation 3 Gaussian	actual para	0.050	0.100	0.005	0.200	NA
	3-para	0.046 (0.001)	0.100 (0.003)	0.008 (0.001)	NA	-474.2
	4-para Gaussian	0.048 (0.001)	0.090 (0.003)	0.005 (0.001)	0.226 (0.006)	-495.3
	4-para gamma	0.048 (0.001)	0.071 (0.002)	0.005 (0.001)	0.339 (0.005)	-478.9
Simulation 4 Gaussian	actual para	0.050	0.100	0.005	0.300	NA
	3-para	0.045 (0.001)	0.111 (0.004)	0.009 (0.001)	NA	-440.9
	4-para Gaussian	0.048 (0.001)	0.097 (0.004)	0.005 (0.001)	0.264 (0.022)	-482.5
	4-para gamma	0.048 (0.001)	0.082 (0.003)	0.004 (0.001)	0.367 (0.004)	-471.4
Simulation 5 Gaussian	actual para	0.050	0.100	0.005	0.350	NA
	3-para	0.042 (0.001)	0.117 (0.004)	0.014 (0.002)	NA	-478.0

	4-para Gaussian	0.046 (0.001)	0.107 (0.004)	0.008 (0.001)	0.273 (0.020)	-517.1
	4-para gamma	0.047 (0.001)	0.089 (0.003)	0.007 (0.001)	0.379 (0.006)	-491.1
Simulation 6 Gaussian	actual para	0.050	0.100	0.005	0.400	NA
	3-para	0.037 (0.001)	0.096 (0.005)	0.017 (0.002)	NA	-471.4
	4-para Gaussian	0.040 (0.001)	0.085 (0.005)	0.012 (0.002)	0.271 (0.021)	-509.1
	4-para gamma	0.044 (0.001)	0.078 (0.002)	0.005 (0.001)	0.401 (0.010)	-455.5
Simulation 7 Gaussian	actual para	0.050	0.100	0.005	0.500	NA
	3-para	0.036 (0.001)	0.108 (0.005)	0.019 (0.002)	NA	-453.9
	4-para Gaussian	0.040 (0.001)	0.098 (0.005)	0.014 (0.002)	0.277 (0.020)	-478.8
	4-para gamma	0.045 (0.001)	0.078 (0.006)	0.006 (0.001)	0.481 (0.001)	-469.2
Simulation 8 gamma	actual para	0.050	0.100	0.005	0.400	NA
	3-para	0.044 (0.001)	0.120 (0.005)	0.012 (0.002)	NA	-455.3
	4-para Gaussian	0.048 (0.001)	0.109 (0.005)	0.005 (0.002)	0.285 (0.005)	-498.5
	4-para gamma	0.048 (0.001)	0.087 (0.006)	0.005 (0.002)	0.395 (0.002)	-499.4
Simulation 9 gamma	actual para	0.050	0.100	0.005	0.500	NA
	3-para	0.036 (0.001)	0.126 (0.005)	0.020 (0.007)	NA	-433.7
	4-para Gaussian	0.046 (0.001)	0.130 (0.005)	0.005 (0.002)	0.324 (0.005)	-444.3
	4-para gamma	0.047 (0.001)	0.093 (0.007)	0.005 (0.002)	0.504 (0.002)	-470.8
Simulation 10	actual para	0.050	0.100	0.005	0.577	NA

gamma	3-para	0.034 (0.005)	0.124 (0.022)	0.022 (0.007)	NA	-463.6
	4-para Gaussian	0.039 (0.001)	0.117 (0.007)	0.015 (0.002)	0.286 (0.007)	-490.2
	4-para gamma	0.044 (0.001)	0.062 (0.007)	0.008 (0.003)	0.585 (0.004)	-491.0
Simulation 11 gamma	actual para	0.050	0.100	0.005	0.632	NA
	3-para	0.028 (0.006)	0.133 (0.026)	0.026 (0.008)	NA	-422.2
	4-para Gaussian	0.035 (0.006)	0.125 (0.027)	0.018 (0.008)	0.294 (0.001)	-438.4
	4-para gamma	0.046 (0.001)	0.078 (0.008)	0.004 (0.002)	0.640 (0.006)	-464.4
Simulation 12 gamma	actual para	0.050	0.100	0.005	0.707	NA
	3-para	0.022 (0.008)	0.143 (0.044)	0.032 (0.009)	NA	-497.6
	4-para Gaussian	0.023 (0.008)	0.115 (0.044)	0.035 (0.009)	0.268 (0.001)	-512.8
	4-para gamma	0.049 (0.001)	0.093 (0.009)	0.005 (0.002)	0.712 (0.004)	-513.1